

## Experimental determinations of universal amplitude combinations for binary fluids. I. Statics

D. Beysens, A. Bourgou, and P. Calmettes

*Commissariat à l'Energie Atomique, Division de la Physique, Service de Physique du Solide et de Résonance Magnétique, B.P. No. 2—91190 Gif-sur-Yvette, France*

(Received 22 January 1982)

The amplitudes of the correlation length ( $\xi_0^+$ ,  $\xi_0^-$ ) and ( $\xi_0^+$ ) on the critical isotherm, the susceptibility ( $C^+$ ,  $C^-$ ) and ( $D$ ) on the critical isotherm, the order parameter ( $B$ ), and the specific heat ( $A^+$ ,  $A^-$ ), have been obtained for eight binary fluids in the homogeneous (+) or the heterogeneous region (-). All the values have been inferred using the universal values of critical exponents. An accurate approximation for the correlation function, which however does not include corrections to scaling, has been used to deduce  $\xi_0^+$  and  $C^+$  from light scattering measurements. Spectral analysis of the scattered light allows absolute values of  $C^+$  to be obtained from the Rayleigh-Brillouin ratio without any assumptions concerning the Rayleigh factor expression. The critical anomaly of the refractive index has been used in several cases to estimate the specific-heat anomaly. Values have been obtained for height amplitude combinations,  $A^+/A^-$ ,  $C^+/C^-$ ,  $\xi_0^+/\xi_0^-$ ,  $R_c^+ = A^+C^+/B^2$ ,  $R_\chi^+ = C^+DB^{\delta-1}$ ,  $R_\xi^+ = \xi_0^+(A^+)^{1/3}$ ,  $R_\xi^+(R_c^+)^{-1/3} = \xi_0^+(B^2/C^+)^{1/3}$ , and  $Q_2 = (C^+/C_c)(\xi_0^+/\xi_0^+)$ . The universality of these ratios is well supported, and the values found are in agreement with those given by the high-temperature series and the renormalization-group approaches. The experimental values of  $C^+/C^-$  and  $R_\xi^+$  are found to be closer to the renormalization-group prediction.

### I. INTRODUCTION

In the field of phase transitions, particular attention has been paid over the last ten years to the exponents involved in the scaling laws which describe the asymptotic behavior of any system near the critical point. These exponents have been shown<sup>1</sup> to be universal for any given class of systems: they are functions only of the dimensionality of the physical space and of the number of the components of the order parameter. However, some recent theoretical<sup>2-7</sup> and experimental works<sup>8-12</sup> have also been devoted to the universal relationships connecting the leading amplitudes, and to the amplitudes of the correlations to scaling.<sup>13-16</sup>

This paper is concerned only with binary fluids, which belong to the same class as the three-dimensional Ising model. From an experimental point of view, numerous data can be found concerning critical exponents,<sup>11,12</sup> but the measurements of both the amplitudes and the corrections to scaling are very scarce. Moreover, most of these measurements suffer from a lack of accuracy which prevents any conclusions from being made. Apart from the accuracy of the measurements, the

most important possible origin of errors is the high sensitivity of both the amplitudes and the critical temperature  $T_c$  to any impurities, which however do not greatly affect the values of the exponents. Therefore the chemical purity of the system is very important, and any possible contamination during the experiment must be avoided. As far as possible, the different amplitudes should consequently be measured in the same sample.

The purpose of this paper is to evaluate the critical amplitudes required for the calculation of some of the universal amplitude relationships. The values of these amplitudes are inferred from both new measurements and new analyses of old measurements. Eight binary mixtures have been investigated, and only the leading static amplitudes are considered here. Further papers will be devoted to dynamic amplitude relationships and to scaling corrections.

Section II of this work presents a rapid survey of the theoretical situation. Section III is concerned with the determination of the correlation length and of the susceptibility, including new data and analyses by turbidity measurements and Rayleigh-Brillouin ratios. Section IV is devoted to

the specific-heat amplitudes. New analyses of calorimetry and volume measurements are provided, and new data concerning refractive index measurements are given. Section V deals with the order parameter, for which new analyses of existing data are performed. Finally, in Sec. VI, all previous results are used to calculate some of the leading amplitude ratios. In order to simplify the reading of this paper, the presentation of the experimental aspects of this work is given in a number of appendices.

## II. THEORETICAL BACKGROUND

The quantities which have been experimentally determined are the correlation length, the susceptibility, the order parameter, and the specific heat. For all these above quantities  $f_j(t)$ , the behavior versus the reduced temperature  $t = |(T - T_c)/T_c|$  ( $T = T_c$  is the critical absolute temperature) can be described near  $T_c$  as

$$f_j^\pm(t) |_{t \rightarrow 0^\pm} = f_j^\pm(0) t^{-\lambda_j} (1 + a_{jj}^\pm t^\Delta + \dots) + f_{j,R}^\pm. \quad (1)$$

$+$  ( $-$ ) denotes the homogeneous (heterogeneous) region.  $\lambda_j$  are critical exponents,  $f_j^\pm(0)$  are the corresponding leading amplitudes,  $a_{jj}^\pm$  are the amplitudes of the first-order correction-to-scaling contributions with critical exponent  $\Delta \simeq 0.50$ , and  $f_{j,R}^\pm$  represents the nonsingular terms.

### A. Correlation length $\xi$

For a binary system at the critical concentration, the correlation length can be written as

$$\xi^\pm = \xi_0^\pm t^{-\nu} (1 + a_\xi^\pm t^\Delta + \dots) + \xi_R^\pm. \quad (2)$$

$\nu = 0.630$  (Refs. 1, 17–19) is the universal exponent and  $\xi_0^\pm$  the corresponding amplitude. In binary mixtures the presence of  $\xi_R^\pm$  has never been detected. Typically  $\xi_0^\pm$  ranges from 1 to 4 Å, and the correction  $a_\xi^\pm$  has not yet been directly measured, presumably because most static determinations are performed very close to  $T_c$ .

Light scattering measurements are able to give values for  $\xi$  as will be explained below.

### B. Susceptibility $\chi$

The susceptibility in binary fluids is the reduced osmotic compressibility  $\chi = k_B T_c / (\partial\mu / \partial c)_{p,T}$ ,

where  $\mu$  is the difference between suitable chemical potentials of the components,  $p$  is pressure,  $k_B$  is the Boltzmann constant, and  $i$  is the “proper” concentration (see below):

$$\chi^\pm = C^\pm t^{-\gamma} (1 + a_\chi^\pm t^\Delta + \dots) + \chi_R^\pm, \quad (3)$$

where  $\chi_R^\pm$  is a possible regular contribution which has not been evidenced.  $\gamma = 1.240$  (Refs. 1 and 17–19) is the corresponding universal exponent. Typically  $k_B T_c C^{-1} = (\partial\mu / \partial c)_{p,T}^0 \simeq 50 - 200 \text{ J cm}^{-3}$ ;  $a_\chi^\pm$  is generally not visible. As for  $\xi$ , light scattering techniques allow  $\chi$  to be obtained.

### C. Specific heat $C_{p,i}$

The specific heat at constant pressure and concentration corresponds in binary fluids to the specific heat at constant volume in pure fluids, and exhibits the same weak divergence with the exponent  $\alpha = 0.110$  (Refs. 1 and 17–19):

$$\frac{C_{p,i}^\pm}{k_B} = \frac{A^\pm}{\alpha} t^{-\alpha} (1 + \alpha a_c^\pm t^\Delta + \dots) + C_R^\pm. \quad (4)$$

Generally a large regular part is found in binary fluids. Most experiments did not report correction-to-scaling terms. The value of  $A$  can vary by a factor of 20, from 0.5 to  $10 (\times 10^{-21} \text{ cm}^{-3})$ .

### D. Order parameter $M$

In binary mixtures the order parameter  $M$  is the difference  $M^{u,l} = i^{u,l} - i_c$  of the concentration  $i^{u,l}$  of one component and its critical value  $i_c$ . ( $u$ ) or ( $l$ ) refers to the phase above or below the meniscus, in a gravity field. It is convenient to separate the variation of  $M$  into parts which are expected to show the following behaviors:

$$\begin{aligned} \Delta M &= |M^u - M^l| / 2 \\ &= B t^\beta (1 + a_m t^\Delta + \dots), \end{aligned} \quad (5)$$

where  $B$  is the amplitude of the coexistence curve, and  $\beta = 0.325$  (Refs. 1 and 17–19). Then

$$\langle M \rangle = \frac{M^u + M^l}{2}$$

is the so-called diameter of the coexistence curve.

A problem in binary fluids (as in pure fluids) is that the proper order parameter is not known, and therefore either mass fraction, molar fraction, volume fraction, etc., can be used as a first-order

approximation. This may have an incidence on the amplitudes and correction-to-scaling terms and complicates the behavior of  $\langle M \rangle$ , which can exhibit terms in  $t^{1-\alpha}$ ,  $t^{2\beta}$ , in addition to linear and correction-to-scaling contributions.<sup>20</sup> We will therefore write  $\langle M \rangle$  as

$$\langle M \rangle = M_c (1 + m_1 t + m_2 t^{1-\alpha} + m_2' t^{2\beta} + \dots)(1 + \dots), \quad (6)$$

where the second ellipsis means corrections.

### E. Critical isotherm

The critical isotherm ( $t=0$ ) equation is

$$\mu = DM^\delta (1 + \dots) \quad (7)$$

with  $\delta = \gamma/\beta + 1 = 4.815$  the universal exponent. The susceptibility behaves as

$$k_B T \chi = C_c \mu^{-\gamma/\beta\delta} \equiv \frac{1}{\delta D^{1/\delta}} \mu^{-\gamma/\beta\delta} \quad (8)$$

and the correlation length

$$\xi^c = \xi_0^c \mu^{-\nu/\beta\delta}. \quad (9)$$

Here we have omitted the correction-to-scaling terms. It is worth noticing that up to the Ref. 21 work, no experimental data were available in binary mixtures along the critical isotherm.

### F. Amplitude combinations

There are three kinds of amplitude relationships as follows:

(i) Ratio of amplitudes in both homogeneous and heterogeneous regions, such as  $A^+/A^- \simeq 0.5$ ,  $\xi_0^+/\xi_0^- \simeq 2$ , and  $C^+/C^- \simeq 4.5$ . The universality of the ratio results from the equality of exponents above or below  $T_c$ .

(ii) Relations between "thermodynamic" amplitudes resulting from the relations between critical exponents. Here the ratio  $R_c^+ = C^+ A^+ / B^2 \simeq 0.06$  and  $R_\chi^+ = C^+ D B^{\delta-1} \simeq 1.7$  will be studied.

(iii) Relations between thermodynamic and the correlation length amplitudes. Hyperscaling, which relates the space dimensionality  $d$  to  $\alpha$  and  $\nu$  by  $d\nu = 2 - \alpha$ , directly leads to the universality of

$$R_\xi^+ = \xi_0^+ (A^+)^{1/3} \simeq 0.25 - 0.027.$$

An interesting relationship is also

$$Q_2 = \frac{C^+}{C_c} \left[ \frac{\xi_0^c}{\xi_0^+} \right]^{2-\eta} \simeq 1.2.$$

(iv) Another relation, which is a combination of  $R_c^+$  and  $R_\xi^+$ , is of interest since it is more easily experimentally measured

$$R_\xi^+ R_c^{-1/3} = \xi_0^+ (B^2/C^+)^{1/3} \simeq 0.65 - 0.67.$$

We will now review and discuss the techniques and the data concerning the above amplitudes.

## III. CORRELATION LENGTH AND SUSCEPTIBILITY: LIGHT SCATTERING

Scattered light intensity measurements allow the static structure factor  $S(X)$  to be determined.<sup>22</sup>

Here  $X = q\xi$ , where  $q$  is the transfer wave vector, and a wide range of values can be easily achieved for  $X$ : typically  $10^{-3} \leq X \leq 30$ . Since  $S(X)$  is essentially the Fourier transform of the normalized correlation function  $G(X)$  multiplied by the order parameter susceptibility  $\chi$ , values for  $\chi$  and  $\xi$  can be obtained.

However, a good model of the correlation function  $G(X)$  has to be known. We shall not discuss here the case where corrections to scaling are important (see Ref. 16); these corrections should modify to some extent the functional form of  $G(X)$ . The scaling correlation function proposed by Bray<sup>23,24</sup> seems up to now the most appropriate scaling function for systems which belong to the same class as the three dimensional (3D) Ising model. Both for  $X \ll 1$  and  $X \gg 1$ , the functional asymptotic form of  $G(X)$  can be regarded as theoretically well known.<sup>25</sup> On the contrary, the correlation function  $G(X)$  has to be determined numerically when  $X \simeq 1$ . Consequently, an analytical approximation has been developed from the numerical values reported in Ref. 24. This approximation is

$$G(X) = \sum_{j=1}^3 c_j (1 + a_j^2 X^2)^{-b_j} \quad (10)$$

with  $c_1 = c_2 = 1$ ,  $c_3 = -1$ ;  $a_1 = 1.040056$ ,  $a_2 = 1.058947$ ,  $a_3 = 1.053932$ ;  $b_1 = 1 - \eta/2 = 0.98425$ ,  $b_2 = 1.554213$ ,  $b_3 = 1.627419$ .  $\eta$  is the Fisher exponent whose theoretical value is 0.0315.<sup>1,17-19</sup> In Table I, the numerical values of this approximation are given for  $\nu = 0.630$ , together with the data of Ref. 24. The deviations between them are indeed very small.

### A. Scattered light intensity

The intensity of the light scattered by the concentration fluctuations of a binary mixture near the

TABLE I. An approximation for the correlation function  $G(X) = \sum_{i=1}^3 c_i (1 + a_i^2 X^2)^{-b_i}$ , with  $a_1 = 1.040056$ ,  $a_2 = 1.058947$ ,  $a_3 = 1.053932$ ,  $b_1 = 1 - \eta/2 = 0.98425$ ,  $b_2 = 1.554213$ ,  $b_3 = 1.627419$ ,  $c_1 = c_2 = 1$ ,  $c_3 = -1$ .  $D-01$  means  $10^{-1}$ .

| $X$          | Data <sup>a</sup> | $G(X)$          | Absolute deviation |
|--------------|-------------------|-----------------|--------------------|
| 0.0          | 1.000 000 0D-00   | 1.000 000 0D 00 | 2.220 45D-16       |
| 1.000 00D-01 | 9.901 000 0D-01   | 9.901 007 7D-01 | -7.721 88D-07      |
| 1.258 90D-01 | 9.844 000 0D-01   | 9.844 018 1D-01 | -1.809 99D-06      |
| 1.584 90D-01 | 9.755 000 0D-01   | 9.755 010 9D-01 | -1.088 66D-06      |
| 1.995 30D-01 | 9.617 300 0D-01   | 9.617 198 2D-01 | 1.018 29D-05       |
| 2.511 90D-01 | 9.406 700 0D-01   | 9.406 613 8D-01 | 8.619 85D-06       |
| 3.162 30D-01 | 9.091 200 0D-01   | 9.091 116 3D-01 | 8.372 00D-06       |
| 3.981 19D-01 | 8.632 400 0D-01   | 8.632 284 9D-01 | 1.151 45D-05       |
| 5.011 90D-01 | 7.993 100 0D-01   | 7.992 997 4D-01 | 1.026 13D-05       |
| 6.309 60D-01 | 7.153 500 0D-01   | 7.153 485 2D-01 | 1.476 73D-06       |
| 7.943 30D-01 | 6.132 700 0D-01   | 6.132 789 5D-01 | -8.952 44D-06      |
| 1.000 00D-00 | 5.001 700 0D-01   | 5.001 906 3D-01 | -2.063 37D-05      |
| 1.258 90D-00 | 3.870 600 0D-01   | 3.871 014 0D-01 | -4.140 47D-05      |
| 1.584 90D 00 | 2.849 800 0D-01   | 2.849 961 0D-01 | -1.610 34D-05      |
| 1.995 30D 00 | 2.010 100 0D-01   | 2.010 122 1D-01 | -2.206 79D-06      |
| 2.511 90D 00 | 1.370 600 0D-01   | 1.370 628 5D-01 | -2.850 89D-06      |
| 3.162 30D 00 | 9.116 500 0D-02   | 9.115 881 1D-02 | 6.189 420-06       |
| 3.981 10D 00 | 5.959 500 0D-02   | 5.958 937 5D-02 | 5.624 95D-06       |
| 5.011 90D 00 | 3.851 100 0D-02   | 3.850 757 3D-02 | 3.426 66D-06       |
| 6.309 60D 00 | 2.470 200 0D-02   | 2.470 127 1D-02 | 7.294 95D-07       |
| 7.943 30D 00 | 1.577 200 0D-02   | 1.577 260 9D-02 | -6.092 18D-07      |
| 1.000 00D 01 | 1.004 300 0D-02   | 1.004 372 0D-02 | -7.199 16D-07      |
| 1.258 90D 01 | 6.385 000 0D-03   | 6.385 802 5D-03 | -8.025 34D-07      |
| 1.584 90D 01 | 4.056 000 0D-03   | 4.056 289 3D-03 | -2.893 38D-07      |
| 1.995 30D 01 | 2.575 600 0D-03   | 2.575 571 1D-03 | 2.885 19D-08       |
| 2.511 90D 01 | 1.635 300 0D-03   | 1.635 226 4D-03 | 7.358 01D-08       |
| 3.162 30D 01 | 1.038 300 0D-03   | 1.038 169 8D-03 | 1.301 82D-07       |

<sup>a</sup> $\nu = 0.630$  and  $\eta = 0.315$ , from Ref. 24.

critical point can be written in the following form<sup>22,26</sup>:

$$I_S = \frac{\pi^2}{\lambda_0^4} S_n^2 \left[ \frac{\partial n^2}{\partial i} \right]^2 G(X) \left[ \frac{\partial \mu}{\partial i} \right]_{p,T}^0 t^{-\gamma(1 + \dots)}, \quad (11)$$

where the ellipsis represents corrections to scaling, and where  $\lambda_0$  is the wavelength of light in vacuum. The quantity  $S_n$  reflects the coupling between the scattered electric field and the concentration fluctuations;  $S_n = 1$ ,  $S_n = 9n^2/(n^2 + 2)(2n^2 + 1)$ , or  $S_n = 3/(n^2 + 2)$  according to Einstein's, Yvon's, or

Rocard's theories, respectively. The parameter  $(\partial n^2/\partial i)_{p,T}$  is the usual bulk derivative, which can be approximated by the Lorentz-Lorenz formula.<sup>27,28</sup> For pure fluids, the experimental results agree equally well with the assumptions of Yvon and Rocard.<sup>27-30(a)</sup> Einstein's result is generally beyond the measurement accuracy. For binary mixtures, Yvon's theory seems to describe the experimental results better than does Rocard's theory.<sup>28</sup>

The temperature and wave-vector dependence of the scattered light intensity allows one to determine the exponents  $\gamma$ ,  $\nu$  and the amplitude  $\xi_0$  of the correlation length. Table II gives the values of  $\xi_0$  obtained in this way for the mixtures ni-

TABLE II. Amplitudes of the correlation length and of the susceptibility obtained by different techniques.  $\nu$  and  $\gamma$  are the values adopted for the fits.

| Systems | Measurements                    | $\xi_0(\text{\AA})$ | $\nu$             | $\gamma$          | $\frac{\left(\frac{\partial\mu}{\partial i}\right)^0_{p,T}}{S_n^2 \left(\frac{\partial n^2}{\partial i}\right)^2_{p,T}} (\text{J cm}^{-3})$<br>$\lambda = 6328\text{\AA}$ | $\frac{\left(\frac{\partial\mu}{\partial i}\right)^0_{p,T}}{\left(\frac{\partial n^2}{\partial i}\right)^2_{p,T}} (\text{J cm}^{-3})$<br>$\lambda = 6328\text{\AA}$ |
|---------|---------------------------------|---------------------|-------------------|-------------------|---|---|
| A-C     | Turbidity <sup>c</sup>          | $2.45 \pm 0.05$     | 0.630             | 1.240             |   |   |
| N-I     | Rayleigh-Brillouin <sup>f</sup> | $2.42 \pm 0.04$     | 0.630             | 1.240             | $(5.3 \pm 0.1) \times 10^2$   | $\left\{ \begin{array}{l} (7.4 \pm 0.1) \times 10^{6g} \\ (2.68 \pm 0.4) \times 10^{6h} \end{array} \right.$  |
| T-W     | Turbidity <sup>a</sup>          | $1.28 \pm 0.05$     | 0.630             | 1.240             | $(6.23 \pm 0.20) \times 10^3$   |   |
|         | Turbidity <sup>j</sup>          | $1.0 \pm 0.1$       | ?                 | ?                 |   |   |
| T-D     | Turbidity <sup>b</sup>          | $1.08 \pm 0.1$      | ?                 | ?                 |   |   |
| I-W     | Turbidity <sup>c,m</sup>        | $3.625 \pm 0.065$   | 0.630             | 1.240             | $(1.48 \pm 0.27) \times 10^3$   |   |
| N-M     | Turbidity <sup>c,k</sup>        | $2.38 \pm 0.30$     | 0.630             | 1.240             | $(5.9 \pm 1.3) \times 10^4$   |   |
|         | Scattered light <sup>l</sup>    | $2.16 \pm 0.03$     | 0.630             | 1.240             |   |   |
| N-H     | Rayleigh-Brillouin <sup>d</sup> | $1.4 \pm 0.1^n$     | 0.630             | 1.240             | $\left\{ \begin{array}{l} (1.37 \pm 0.05) \times 10^{2n} \\ (5.9 \pm 0.1) \times 10^{2o} \end{array} \right.$   | $(5.2 \pm 0.5) \times 10^2$   |
|         | Turbidity <sup>d</sup>          | $2.65 \pm 0.07^o$   |                   |                   |   |   |
|         | Scattered light <sup>e</sup>    | $3.64 \pm 0.22$     |                   |                   |   |   |
| C-P     | Turbidity <sup>c,l</sup>        | $2.40 \pm 0.20$     | 0.630             | 1.240             | $(6.00 \pm 0.33) \times 10^2$   |   |
|         | Scattered light <sup>l</sup>    | $2.28 \pm 0.21$     | $0.626 \pm 0.013$ | $1.220 \pm 0.018$ |   |   |

<sup>a</sup>Reference 31.

<sup>b</sup>Cited in Ref. 35.

<sup>c</sup>Appendix A.

<sup>d</sup>Reference 21.

<sup>e</sup>Reference 59.

<sup>f</sup>Reference 26.

<sup>g</sup> $\lambda = 6328 \text{\AA}$ .

<sup>h</sup> $\lambda = 4880 \text{\AA}$ .

<sup>i</sup>Reference 24.

<sup>j</sup>Cited in Ref. 38.

<sup>k</sup>Reference 32.

<sup>l</sup>Reference 33.

<sup>m</sup>Reference 60.

<sup>n</sup> $T < T_c$ .

<sup>o</sup> $T > T_c$ .

troethane and 3-methylpentane (N-M), nitrobenzene-*n*-hexane (N-H), and carbon tetrachloride and perfluoromethyl cyclohexane (C-P). The corresponding values of  $\gamma$  and  $\nu$  are also given.

As far as the amplitude of  $\chi$  is concerned, it is necessary to measure the absolute value of the scattered light intensity  $I_S$ . Practically, it is quite impossible to perform such measurements with a sufficient accuracy, mainly because the geometry of the experiment is generally not well known. However, the ratio of scattered intensities from different spectral contributions is independent of most of the above factors.

### B. Rayleigh-Brillouin ratio

The spectral analysis of the light scattered from a binary fluid allows the contribution from the concentration fluctuations to be separated from the contribution arising from pressure fluctuations. These fluctuations give rise to the Brillouin lines,

which are frequency shifted with respect to the concentration line (Fig. 1). As stressed above, the value of  $S_n$  in the expression of the scattered light intensity is still subject to controversy; however  $S_n^2$  appears as a multiplicative factor in the expression of the Brillouin lines intensity. This is merely because the local field expressions do not depend on the nature of the fluctuation which gives rise to the scattered electric field. Therefore the ratio  $R/2B$  of the frequency integrated intensities is no longer a function of  $S_n$ , and can be written as

$$\frac{R}{2B} = \frac{\left[ \frac{\left(\frac{\partial n^2}{\partial i}\right)_{p,T}}{\left(\frac{\partial \mu}{\partial i}\right)_{p,T}} \right]^2}{\left[ \frac{\rho \frac{\partial n^2}{\partial \rho}}{\left(\frac{\partial \mu}{\partial i}\right)_{p,T}} \right]} t^{-\gamma G(X)}, \quad (12)$$

with  $V_{HF}$  the sound velocity at the Brillouin frequency. From the variations of  $R/2B$  with  $t$  at fixed  $q$ , both the exponents  $\gamma$  and  $\nu$  and the amplitudes  $(\partial\mu/\partial i)_{p,T}^0$  and  $\xi_0$  can be inferred.

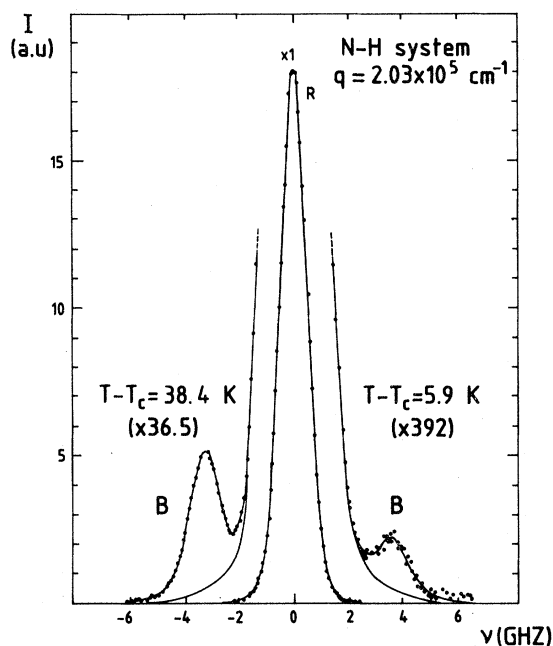


FIG. 1. Spectrum of the light scattered from the nitrobenzene + *n*-hexane system at two different temperatures, showing the strong variation of the central (Rayleigh) peak due to concentration fluctuations. Shifted lines are the Brillouin components due to pressure fluctuations. They exhibit no anomaly near  $T_c$  and can be used as an intensity standard. [Note the change of scale ( $\times 36.5$  and  $\times 392$ ) (from Ref. 21).]

In Ref. 26 a complete analysis of the data obtained for the nitroethane-isooctane (N-I) system is given. Useful final results are reported in Table II.

$$G'(X_0) = \sum_{i=1}^3 c_i \{ [(1 + 2a_i^2 X_0^2)^{\mu_i} - 1] [1 + a_i X_0^2 (2 - \mu_i) + a_i^4 X_0^4 (2 + \mu_i + \mu_i^2)] - 2\mu_i X_0^2 (1 + X_0^2) \} \\ \times [a_i^6 X_0^6 \mu_i (1 + \mu_i) (2 + \mu_i)]^{-1}, \quad (16)$$

where  $a_i$  and  $c_i$  are the same as for  $G(X)$ , and where the  $\mu_i$  are deduced from the  $b_i$  by the relation  $\mu_i = 1 - b_i$ . Note that this formula is the straightforward generalization of the calculation made in Ref. 30(b) with a simpler model for  $G(X)$ .

The fit of this expression (16) to transmission measurements performed at different temperatures, or different values of  $M$  on the critical isotherm using  $t \simeq (M/B)^{1/\beta}$ , can give significant values for the adjustable parameters  $\gamma$ ,  $\nu$  and the amplitudes  $\tau_0$  and  $\xi_0$ . Of course the binary fluid must be sufficiently turbid so that the decrease of the transmission can be easily measurable. Nevertheless, very turbid systems may give erroneous results if

The same kind of results are also available for the N-H system.<sup>21</sup>

### C. Turbidity

Near the critical point, the scattered intensity may become so important that the transmission of light through the sample decreases. From the turbidity  $\tau$  (rate of decrease of the light intensity per unit length), the same quantities as above can therefore be inferred. If  $l$  is the light path in the sample, the light transmission is

$$\mathcal{E} = \exp[-(\tau + \alpha_0)l], \quad (13)$$

where  $\alpha_0$  is the regular absorption. The turbidity  $\tau$  is the scattered intensity integrated over a solid angle  $4\pi$ , and can be written as

$$\tau = \tau_0 (1 + t) t^{-\gamma} G'(X_0), \quad (14)$$

with

$$\tau_0 = \frac{2\pi^3}{\lambda_0^4} S_n^2 \left[ \frac{\partial n^2}{\partial i} \right]_{p,T}^2 \frac{k_B T_c}{\left[ \frac{\partial \mu}{\partial i} \right]_{p,T}^0}. \quad (15)$$

In this expression the uncertainty concerning the local field value is again reflected by the quantity  $S_n$ .  $G'(X_0)$  is directly deduced from the solid-angle integration of  $G(X)$ . With  $X_0 = \sqrt{2} K_0 \xi$ , where  $K_0 = 2\pi n / \lambda_0$  is the wave vector of incident light,

the light path in the medium is too long.

This turbidity technique is very simple to set up, and we have used it to investigate four different systems, aniline and cyclohexane (A-C), isobutyric acid + water (I-W), N-H, and triethylamine and water (T-W).<sup>31</sup> We have analyzed the corresponding data, and other data already published concerning the systems N-M (Ref. 32) and C-P.<sup>33</sup> The experimental set-up, the data, and their analysis can be found in Appendix A. The final results are listed in Table II.

One can notice the correct agreement for the  $\xi_0$  values obtained in the same sample using scattered light and turbidity measurements for the

N-M and C-P systems. On the contrary, when samples from different origins have been used, the agreement between the two techniques is poorer (N-H and T-W systems). The probable explanation for the discrepancy could be the different origin of the components. As already stressed, the amplitude values are very sensitive to the amount and to the nature of the present impurities. For instance, Ref. 34 reports measurements of  $\xi_0$  in the N-M mixture using pure nitroethane (1) and nitroethane with 3% impurity (2), mainly water. The correlation length amplitude was seen to increase from  $\xi_0 = 2.26 \text{ \AA}$  (1) to  $3.25 \text{ \AA}$  (2), i.e., to show a variation of 40%.

#### IV. SPECIFIC HEAT

Owing to the smallness of the exponent  $\alpha$ , and the generally important value of the regular part of the specific heat at constant pressure and concentration, both exponents and amplitudes are very difficult to estimate from measurements. Several techniques have been used.

##### A. Calorimetry

The basis principle of calorimetry consists in measuring the temperature rise  $\Delta t$  associated to the supply of a given power

$$\Delta H = \int_{t_0}^{t_1} C_{p,i} dt \propto t_1^{1-\alpha} + \text{const} \quad (17)$$

and it is therefore the exponent  $(1-\alpha)$  rather than the exponent  $\alpha$  which is measured.<sup>35</sup> When temperature increments are very small, one may nevertheless consider  $\Delta H/(t_1 - t_0) \propto t^{-\alpha}$ .

Direct calorimetric measurements of  $C_{p,i}$  have previously allowed the divergence to be detected,<sup>36-38</sup> but the estimations of  $\alpha$  were only qualitative. This seems to be due to both thermal gradients and gravity effects, which can alter the critical behavior of the specific heat. In order to prevent density gradients, a continuous stirring of the sample during the measurement can be regarded as an improvement,<sup>35</sup> but this method can create non-negligible velocity gradients which are now known<sup>39</sup> to strongly distort the critical behavior.

Table III reports calorimetric results concerning the T-W, I-W, C-P, and triethylamine + deuterated water (T-D) mixtures. In Appendix B the data on the I-W system have been reanalyzed assuming  $\alpha = 0.110$ . Note that for the C-P system, the data

have not been reanalyzed and that the value  $\alpha = 0.125$  had been used by the authors. The study of the T-W mixture deserves some remarks. In Ref. 38 a surprisingly high value  $\alpha = 0.25$  was found. When assuming that  $\alpha = 0.125$ , different amplitude values have been deduced,  $A^+ = 56$  with correction-to-scaling terms, and  $A^+ = 40$  without corrections. We have reported in Table III the results of an unpublished analysis with  $\alpha = 0.110$ , as mentioned in Ref. 35.

Also reported are results regarding the two phase region of the T-W and D-W systems. In this region, additional experimental difficulties can cause supplementary artifacts.

##### B. Volume or density measurements

An alternative way to get some information concerning  $C_{p,i}$  comes from the thermodynamic relationship between  $C_{p,i}$  and the thermal expansion coefficient

$$\begin{aligned} \alpha_{p,i} &= \left[ \frac{1}{V} \frac{\partial V}{\partial T} \right]_{p,i} = - \left[ \frac{1}{\rho} \frac{\partial \rho}{\partial T} \right]_{p,i} \\ &= \left[ \frac{C_{p,i} - C_{V,i}}{VT_c} \right] \left[ \frac{dT_c}{dp} \right]_{V,i}, \end{aligned} \quad (18)$$

where  $V$  is volume and  $C_{V,i}$  is the specific heat at constant volume and concentration which is expected to have no critical anomaly in binary fluids.  $(dT_c/dp)_{V,i}$  is the pressure variation of the critical temperature. According to the formula (4), the diverging part of  $\alpha_{p,i}$  should be relatively more important than the  $C_{p,i}$  one since  $C_{V,i}$  is subtracted.

Experimentally a change of volume  $\Delta V$  or density  $\Delta \rho$  is measured when the temperature is varied, and there again it is not the exponent  $\alpha$  which is directly measured, but  $1-\alpha$ :

$$-\Delta \rho \propto \Delta V \propto t^{1-\alpha} + \dots \quad (19)$$

Density or volume measurement can be very accurate. The measurements are performed at thermodynamic equilibrium, but gravity-induced density gradients can affect the results. In addition, external contaminations cannot be completely avoided when the volume variations are studied over a large temperature range. All these reasons could explain why up to now these methods are not able to achieve an accuracy better than  $\pm 70\%$  for  $\alpha$ . Also the choice of the system is very important since both  $A^+$  and  $(dT_c/dp)_{V,i}$  have to be large.

Table III listed the results for the T-W, I-W, N-M, N-H, and C-P systems. Appendix C

TABLE III. Values of the specific heat amplitude  $A^\pm$ , obtained by different techniques.

| System | Measurement                   | $A^+(\times 10^{21} \text{ cm}^3)$ | $A^+/A^-$                | $\alpha$ | $(dT_c/dp)(\times 10^{-8} \text{ K cm}^2 \text{ dy}^{-1})$ | $\left[ \frac{\rho \partial n}{\partial p} \right]_{p,i}$ |
|--------|-------------------------------|------------------------------------|--------------------------|----------|--|---|
| A-C    | Refractive index <sup>a</sup> | 1.2 ± 0.3                          |                          | 0.110    | 0.70 ± 0.05 <sup>b,g</sup>                                 | 0.626 <sup>s</sup>  |
| N-I    | Refractive index <sup>h</sup> | 1.8 ± 0.5                          | 0.56 ± 0.09 <sup>a</sup> | 0.110    | 0.26 ± 0.05 <sup>e</sup>                                   | 0.438 <sup>s</sup>  |
| T-W    | Calorimetry <sup>i</sup>      | 18 ± 3.6 <sup>k</sup>              | 0.63 ± 0.25 <sup>j</sup> | 0.110    |  |   |
|        | Density <sup>l</sup>          | 8.2 ± 0.6                          | 0.36 ± 0.03              | 0.110    | 2.03 ± 0.003 <sup>d</sup>                                  | 0.400 <sup>s</sup>  |
| T-D    | Refractive index <sup>c</sup> | 8.4 ± 0.3                          |                          | 0.110    |  |   |
|        | Calorimetry <sup>l</sup>      | 15.6 ± 0.7                         | 0.57 ± 0.01              | 0.107    |  |   |
| I-W    | Calorimetry <sup>a</sup>      | 0.36 ± 0.02                        |                          | 0.110    |  |   |
|        | Density <sup>m</sup>          | 0.51 ± 0.07                        |                          | 0.125    |  |   |
|        | Volume <sup>n</sup>           | 0.68 ± 0.15 <sup>g</sup>           |                          | 0.110    | -5.20 ± 0.25 <sup>b</sup>                                  | 0.397 <sup>s</sup>  |
| N-M    | Refractive index <sup>c</sup> | 0.46 ± 0.03                        |                          | 0.110    |  |   |
|        | Density <sup>o</sup>          | 3.2 ± 1                            |                          | 0.140    | 0.37 ± 0.05 <sup>e</sup>                                   |   |
| N-H    | Refractive index <sup>p</sup> | 1.05 ± 0.15                        |                          | 0.110    |  |   |
|        | Volume <sup>p</sup>           | 1.19 ± 0.5                         |                          | 0.110    | -1.64 ± 0.08 <sup>b,g</sup>                                | 0.472 ± 0.010 <sup>p</sup>                                |
| C-P    | Calorimetry <sup>q</sup>      | 1.10 ± 0.07                        |                          | 0.125    |  |   |
|        | Density <sup>r</sup>          | 1.10 ± 0.15                        |                          | 0.125    | -4.0 ± 0.16 <sup>f</sup>                                   |   |

<sup>a</sup>Appendix D.<sup>b</sup>Cited in Ref. 61.<sup>c</sup>Reference 46.<sup>d</sup>Reference 62.<sup>e</sup>Reference 63.<sup>f</sup>Reference 64.<sup>g</sup>Uncertainty estimated by us.<sup>h</sup>Reference 40.<sup>i</sup>Reference 38.<sup>j</sup>Reference 38 without corrections to scaling and with  $\alpha=0.125$ .<sup>k</sup>Cited in Ref. 35.<sup>l</sup>Reference 35.<sup>m</sup>Reference 65.<sup>n</sup>Reference 66.<sup>o</sup>Reference 67.<sup>p</sup>Reference 21.<sup>q</sup>Reference 37.<sup>r</sup>Reference 65.<sup>s</sup>Assuming the Lorentz-Lorenz formula.<sup>t</sup>Appendix C.<sup>u</sup>Appendix B.

discusses the analysis of data concerning the T-W mixture in both regions (+ and -).

The agreement between calorimetry and volume or density measurements is good for the I-W and C-P systems, but not for the T-W mixture, where a factor of 2 discrepancy currently exists.

### C. Refractive index measurements

Another method for obtaining information on  $C_{p,i}$  is to measure the refractive index of the mix-

ture. Its variations can be mainly ascribed to the density, and its behavior near  $T_c$  will reflect the critical density anomaly. The experimental interest is obvious since gravity effects are greatly reduced. Indeed the measurement can be made in the sample at the level where composition gradients vanish in the homogeneous phase, i.e., near the middle of the sample height. Furthermore, external contaminations can be completely avoided since the sample can be contained in sealed cells which can be reused for other kinds of measurements.

The only difficulty with this technique lies in



the knowledge of the exact relation between the refractive index and the density. This problem has already been discussed,<sup>40-42</sup> and at the present time two different contributions to the variation  $\Delta n$  of the refractive index are expected:

$$\Delta n = [\Delta\rho] + [\Delta F], \quad (20)$$

where  $[\Delta\rho]$  represents the only contribution from the macroscopic change of density and where  $[\Delta F]$  is the local field modification due to the increasing amplitude of fluctuations.

All contributions can be separated into regular (superscript  $r$ ) and critical (superscript  $c$ ) parts. The critical part  $[\Delta\rho]^c$  of the first term is simply proportional to  $\Delta\rho$  as given by the expressions (18) and (19). The critical contribution  $[\Delta F]^c$  is expected to behave as follows<sup>42,43</sup>:

$$[\Delta F]^c \simeq D_1 t^{-\nu} + D_2 t^{1-\alpha} + \dots \quad (21)$$

Very recently, flow birefringence experiments<sup>44</sup> have ascertained the existence of the first contribution to  $[\Delta F]^c$ , as suggested in Ref. 45, and have shown that within current accuracy it remains negligible near  $T_c$ . The second contribution is expected to be also very small; it is proportional to the coefficient  $(\partial T_c / \partial E^2)$ , with  $E$  the electric field. No experimental verification concerning this single last contribution exists at the present time.

Therefore  $\Delta n$  can be written in the following form:

$$\Delta n = \left[ T_c \frac{\partial n}{\partial T} \right]_{p,i}^{\text{reg}} t + R t^{1-\alpha} + D_2 t^{1-\alpha} + \dots \quad (22)$$

with

$$R = - \left[ \rho \frac{\partial n}{\partial \rho} \right]_{p,i} \left[ \frac{dT_c}{dp} \right]_{v,i} \frac{k_B}{\alpha(1-\alpha)} A. \quad (23)$$

For clarity, the correction-to-scaling terms have been omitted. Note that those related to the  $D_2$  term are not clearly ascertained. The first part represents the regular variation of the refractive index, the second part reflects the critical behavior of the density alone, and the third part corresponds to local field effects.

We will simply neglect this last term in the following, i.e., we will assume that  $R \gg D_2$ . The only available experiments, for T-W, I-W, and N-H systems where both density and refractive index measurements have been made, show that the amplitude of the diverging part of the refractive index can be ascribed to the density alone (see the

$A^\pm$  values given in Table III). Furthermore, we will see later that this assumption does not lead to any inconsistency in the following data analyses, even when correction-to-scaling terms are concerned.<sup>16</sup> Finally, it is worth noticing that this ambiguity does not affect the determination of exponent  $\alpha$ , as determined in Ref. 46.

In Table III the results concerning the A-C, N-I, T-W, I-W, and N-H mixtures are given. In Appendix D, data concerning the A-C and N-I systems (the latter in the inhomogeneous region), have been reported and analyzed. Table III also listed the values of

$$\left[ \rho \frac{\partial n}{\partial \rho} \right]_{p,i} = (n^2 - 1) \frac{(n^2 + 2)}{6n} \quad (24)$$

when one assumes the Lorentz-Lorenz formula. It is well known that this formula (24) is somewhat approximate within a few percent,<sup>47</sup> but it is the only way to determine  $(\rho \partial n / \partial \rho)_{p,i}$  when the analyses of  $n$  and  $\rho$  have not been performed at the same time. This uncertainty is generally much lower than the experimental one.

The results for the T-W mixture deserve some remarks. Contrary to the comments made in Refs. 35 and 48, it seems that no disagreement exists between density and refractive index measurements. Apart from possible experimental artifacts, a possible reason for the present discrepancy between these techniques and calorimetry might be found in the different origin and purity of the components used in this mixture. This could explain why both  $A^+$  and  $\xi_0^+$  disagree with our results, while each value of  $R_\xi^+$  are in agreement (see below).

## V. ORDER PARAMETER

Numerous methods have been used to obtain the coexistence curve of binary mixtures, but they all lead to a "blind" region for  $|T - T_c| \lesssim 0.01$  K where measurements are meaningless. This is due to the flat shape of the curve, which accentuates the influence of external contaminations, gravity effects, very long equilibrium times, etc. Priority will be given to the coexistence curve determination in the same sample used to measure the other diverging quantities. Optical means are very useful since the refractive index is a function of the concentration.

The composition dependence of  $n$  can be expanded in the following<sup>20,42</sup> form:

$$\begin{aligned}
 n_{u,l} = & n_c \pm B_n t^\beta (1 + a_m^- t^\Delta + \dots) \\
 & + R^- t^{1-\alpha} (1 + a_c^- t^\Delta + \dots) \\
 & + Et^{2\beta} + Ft + \dots
 \end{aligned} \quad (25)$$

The subscripts  $u$  ( $l$ ) refer to the upper (lower) phase, corresponding to  $+B_n$  ( $-B_n$ ),  $n_c$  is the refractive index value at  $T_c$ , and the terms  $B_n$ ,  $E$ ,  $F$  are connected to the composition dependence of  $n$ , whereas  $R^-$  represents the contribution of the density and of an eventual local field anomaly.  $R^-$  shows the same functional form as  $R$  in formula (24), neglecting the local field contributions.  $B_n$  is the amplitude of the coexistence curve with  $n$  as an order parameter. It can be related to the amplitude  $B_i$  of the order parameter  $i$  by

$$B_n = B_i \left[ \frac{\partial n}{\partial i} \right]_{p,T} \quad (26)$$

The term  $Et^{2\beta}$  is present whenever the chosen variable is not the "proper" order parameter, and the term  $Ft + \dots$  is expected to represent both the regular contributions of  $n$  and the slope of the coexistence curve diameter. It is worth noticing that this complicated function can be simplified when only the amplitude is concerned:

$$|n_u - n_l| = 2B_n t^\beta (1 + a_m^- t^\Delta + \dots) \quad (27)$$

Careful analyses of the coexistence curves of N-I,<sup>49</sup> T-W,<sup>16,31</sup> and N-H (Ref. 21) (visual and/or refractive-index techniques), and of the I-W system<sup>50</sup> (density measurements), have been recently reported, assuming that  $\beta=0.325$ . The results concerning the amplitudes are given in Table IV. For simplicity, only the variable volume fraction ( $i \equiv \varphi$ ) has been considered. We have also reanalyzed in Appendix E the coexistence curves of the A-C, N-M, N-H, and C-P systems. We have also reported in Table IV the data obtained by a diffraction technique, which is related to the refractive-index variations, and reported a value from the data drawn in Ref. 51 when imposing  $\beta=0.325$ . The difference with the value found in this Reference ( $\beta=0.328$ ) leads to negligible errors.

## VI. AMPLITUDE RELATIONSHIPS

A distinction can be made between the combinations of amplitudes of the same nature ( $A^+/A^-$ ,  $\xi_0^+/\xi_0^-$ ,  $C^+/C^-$ ), the combination of several thermodynamic parameters ( $R_c, R_\chi$ ), and the combinations in which are involved both thermodynamic

TABLE IV. Amplitude of the coexistence curve, with the volume fraction or the refractive index as order parameter.

| System | Measurement                   | $B_\varphi$ | $B_n$  | wavelength<br>(Å) | $\beta$ | $T_c$ (K) |
|--------|-------------------------------|-------------|--|-------------------|---------|-----------|
| A-C    | Density <sup>a</sup>          | 0.97±0.03   | 0.157±0.06   | 6328              | 0.325   | 303       |
|        | Refractive index <sup>b</sup> |             |  |                   | 0.325   |           |
| N-I    | Visual <sup>c</sup>           | 0.885±0.015 | (1.22±0.03)×10 <sup>-3</sup><br>(2.31±0.25)×10 <sup>-3</sup> | 6328<br>4880      | 0.325   | 303       |
|        | Refractive index <sup>c</sup> |             |  |                   | 0.325   |           |
| T-W    | Visual <sup>d</sup>           | 1.605±0.035 | 0.1470±0.0015  | 6328              | 0.325   | 291.5     |
|        | Refractive index <sup>e</sup> |             |  |                   | 0.325   |           |
| I-W    | Density <sup>f</sup>          | 1.071±0.023 |  |                   | 0.328   | 299       |
| N-M    | Density <sup>a</sup>          | 0.852±0.005 |  |                   | 0.325   | 299.5     |
| N-H    | Visual <sup>g</sup>           | 0.770±0.006 | 0.140±0.002  | 6328              | 0.325   | 292.5     |
|        | Refractive index <sup>g</sup> |             |  |                   | 0.325   |           |
| C-P    | Visual <sup>h</sup>           | 0.844±0.013 |  |                   | 0.325   | 301.5     |

<sup>a</sup>Appendix E.

<sup>b</sup>Reference 51.

<sup>c</sup>Reference 49.

<sup>d</sup>Reference 68, reanalyzed in Ref. 31.

<sup>e</sup>References 16 and 31.

<sup>f</sup>Reference 50.

<sup>g</sup>Reference 21.

quantities and the correlation length  
( $R_{\xi}^+$ ,  $R_{\xi}^+ R_c^{-1/3}$ ,  $Q_2$ ).

#### A. Ratios $A^+/A^-$ , $\xi_0^+/\xi_0^-$ , and $C^+/C^-$

Table III lists four values of the ratio  $A^+/A^-$  of the leading amplitudes of the specific heat. The error bars for the T-D measurements seem very low and should be increased when considering the strong concentration gradients which exist in the two phase region, as stressed by the authors.<sup>35</sup>

The theoretical value for  $A^+/A^-$  is 0.51 for high-temperature-series (HTS) computation,<sup>5</sup> and 0.48 for a renormalization-group (RG) calculation<sup>6</sup> up to order  $\epsilon^2$ . From Fig. 2, where both experimental and theoretical values are shown, it can be concluded that the experimental determinations agree relatively well with the theory. It is not possible to decide whether the series of the renormalization group agrees better with the experiments.

Only one value of the ratio  $C^+/C^-$  and  $\xi_0^+/\xi_0^-$  have been obtained, in the N-H system, from turbidity measurements performed above and below  $T_c$ .<sup>21</sup> The  $C^+/C^-$  experimental value is  $4.3 \pm 0.3$ , in very good agreement with the value calculated by an  $\epsilon^2$  expansion in a renormalization-group approach,<sup>4</sup>

$$C^+/C^- = 2^{\gamma-1} \frac{\gamma}{\beta} = 4.5, \quad (28)$$

but not with the HTS estimation of  $5.03 \pm 0.05$ .<sup>4</sup> The ratio  $\xi_0^+/\xi_0^- = 1.9 \pm 0.2$  is in agreement with both the high temperature result 1.96 (Ref. 71) and the renormalization-group calculation 1.91 (Ref. 72).

#### B. Ratio $R_c^+ = A^+ C^+ / B^2$ : Proper order parameter

In this ratio only thermodynamic amplitudes are involved. Its value can be inferred from Tables II, III, and IV. The knowledge of the exact order parameter is important. However, we notice that the ratio  $C^+/B^2$  can be written as a function of the experimental data without making any assumptions on the order parameter: (i) it is not  $C^+$  which is measured, but  $[(\partial n^2/\partial i)_{p,T}^2 / (\partial \mu/\partial i)_{p,T}^0]$ , and (ii) whenever the amplitude of the coexistence curve has been studied by refractive index techniques, the quantity  $B_n = B_i (\partial n/\partial i)_{p,T}$  is known. Therefore  $C^+/B^2$  can be deduced,

$$\frac{C^+}{B^2} = \frac{1}{4n^2} \frac{\left[ \frac{\partial n^2}{\partial i} \right]_{p,T}^2}{\left[ \frac{\partial \mu}{\partial i} \right]_{p,T}^0} \frac{k_B T_c}{B_n^2}. \quad (29)$$

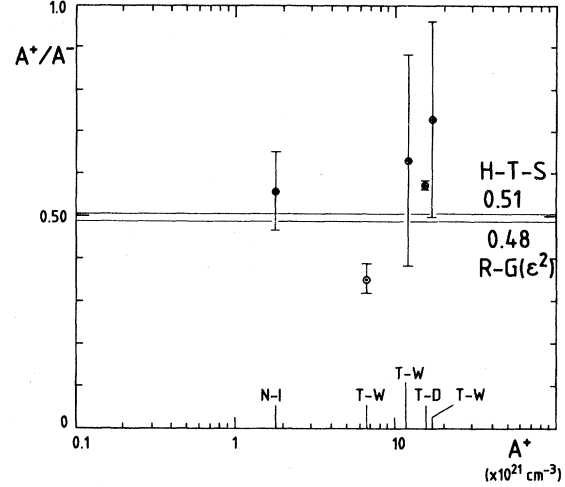


FIG. 2. Ratio  $A^+/A^-$  of the specific-heat amplitudes in the homogeneous (+) and heterogeneous (-) region.  $A^+$  has been chosen as a variable for testing the universality of the ratio. Note the semilogarithmic scale. Three systems were studied, by refractive index (full circle), density (open circle), and calorimetry (crosses). Lines are the theoretical values.

The determination of  $B_n$  has been performed in four systems (C-A, N-I, T-W, and N-H). For the other mixtures only the order parameter, the volume fraction, has been considered and every time the experimental derivative  $(\partial n^2/\partial \varphi)_{p,T}^{\text{exp}}$  was available, it has been preferred to the value calculated by the Lorentz-Lorenz formula for determining  $B_n = (\partial n/\partial \varphi)_{p,T}^{\text{exp}} B_\varphi$ .

However, this relationship is somewhat approximate in the sense that the derivatives  $(\partial n^2/\partial i)_{p,T}$  involved in light scattering and in refractive-index measurements are not the same. In other words there still remains the ambiguity due to the light scattering theories [coefficient  $S_n$  in formula (11)]. As stressed above, the Einstein formulation always gives too high a value, so we have considered only the Yvon-Vuks (Y) or Rocard (R) theories. All systems are concerned, except the N-I and N-H mixtures which have been studied using the Rayleigh-Brillouin ratio technique.

All the  $R_c$  values are listed in Table V. Except for the N-M system, the data are in agreement with the theoretical values 0.059 obtained by HTS,<sup>15</sup> or 0.666 from RG up to order  $\epsilon$ ,<sup>5</sup> as shown in Fig. 3. The accuracy of experimental data is low; this can be attributed to the high number of parameters involved and to the inaccuracy of some  $A^+$  values.

TABLE V. Values of the universal amplitude ratios  $R_c^+ = A^+C^+/B^2$  and  $R_\xi^+ R_c^{-1/3} = \xi_0^+(B^2/C^+)^{1/3}$ . Theoretically expected values are  $R_c = 0.059$  (HTS) or  $0.066$  (RG), and  $R_\xi^+ R_c^{-1/3} = 0.650$  (HTS) or  $0.667$  (RG). Y or R refers to the Yvon-Vuks or Rocard light scattering theories, and RB to the Rayleigh-Brillouin determination of  $C^+$ .

| System | $\left(\frac{\partial n}{\partial \varphi}\right)_{p,T}$<br>( $\lambda$ in $\text{\AA}$ ) | $n$<br>( $\lambda$ in $\text{\AA}$ )   | $Y^a$ |                         | $R_\xi^+ R_c^{-1/3}$ |
|--------|---|--|-------|-------------------------|----------------------|
|        |   |  | $R^b$ | $R_c^+(\times 10^{-2})$ |                      |
| A-C    |   | 1.5242 <sup>(303)</sup> <sub>(6328)</sub>  | { Y   | 5.6±1.7                 | 0.680±0.035          |
| N-I    |   | 1.389 <sup>(303)</sup> <sub>(6328)</sub> <sup>a</sup><br>1.392 <sup>(303)</sup> <sub>(4880)</sub> <sup>b</sup> | { RB  | 8.5±2.9                 | 0.59±0.03            |
|        |   |  |       | 6.8±3.3                 | 0.72±0.07            |
| T-W    |   | 1.3695 <sup>(291.5)</sup> <sub>(6328)</sub> <sup>a</sup>   | { Y   | 4.0±0.4                 | 0.76±0.04            |
|        |   |  |       | R                       | 5.6±0.5              |
| I-W    | $(7.2 \pm 0.7) \times 10^{-2}$<br>(6563) <sup>c,d</sup>                                   | 1.3568 <sup>(299)</sup> <sub>(6328)</sub>  | { Y   | 3.5±1.4                 | 0.86±0.14            |
|        |   |  |       | R                       | 4.9±1.9              |
| N-M    | $(1.48 \pm 0.1) \times 10^{-2}$<br>(6328) <sup>d,e,f</sup>                                | 1.3803 <sup>(299.5)</sup> <sub>(6328)</sub> <sup>e,f</sup>   | { Y   | 23 ± 15                 | 0.53±0.06            |
|        |   |  |       | R                       | 30 ± 20              |
| N-H    | 0.183±0.02 <sup>g</sup>   | 1.444 <sup>(292.5)</sup> <sub>(6328)</sub> <sup>g</sup>  | { Y   | 5.8±1.4                 | 0.68±0.05            |
|        |   |  |       | R                       | 8.5±2.0              |
| C-P    | 0.177<br>(5890) <sup>h,f</sup>  | 1.3673 <sup>(301.5)</sup> <sub>(6328)</sub> <sup>h</sup>   | { RB  | 5.0±1.5                 | 0.73±0.05            |
|        |   |  |       | Y                       | 5.4±0.8              |
|        |   |  | { R   | 7.6±1.1                 | 0.59±0.07            |

<sup>a</sup>Reference 46.

<sup>b</sup>Reference 26.

<sup>c</sup>Reference 61, experimental value.

<sup>d</sup>We have estimated the uncertainty.

<sup>e</sup>Reference 47.

<sup>f</sup>Using the Lorentz-Lorenz formula.

<sup>g</sup>Reference 21.

<sup>h</sup>Reference 33.

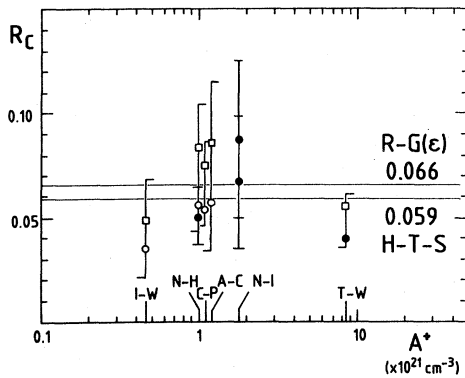


FIG. 3. Combination  $R_c = A^+C^+/B^2$ , as a function of  $A^+$  for checking universality. Note the semilogarithmic scale. Six systems have been investigated. Open circles refer to the  $C^+$  values corresponding to the light scattering theory of Yvon-Vuks, open squares to the Rocard theory. Full circles refer to the  $C^+$  value obtained from the Rayleigh-Brillouin ratio. Lines are the theoretical values.

### C. Ratio $R_\chi^+ = C^+DB^{\delta-1}$

In Ref. 21, the ratio  $R_\chi^+$  have been estimated in the Nitrobenzene-*n* Hexane mixture to  $1.75 \pm 0.30$ , i.e., in excellent agreement with the *R-G* value  $1.7^{19}$ .

### D. Ratio $R_\xi^+ = \xi_0^+(A^+)^{1/3}$

This ratio, which connects thermodynamic and correlation amplitudes directly, comes from the hyperscaling relationship  $d\nu = 2 - \alpha$ , with the space dimensionality  $d = 3$ . This increases the interest of its determination: Hyperscaling has been questionable, for a long time, because it is not satisfied by HTS calculations, but demonstrated by RG theory (however, it has been shown very recently that the HTS approach should also agree with hyperscaling<sup>18-19</sup>). Experimentally, hyperscaling seems to be verified for most binary liquids.<sup>11</sup>

Now, from Tables II and III one can infer  $R_\xi^+$

for eight mixtures. The results are listed in Table VI. As already noticed, we have associated, whenever possible, the amplitudes obtained in the same laboratory. In Fig. 4 these experimental values are compared to the theory  $0.253 \pm 0.001$  from HTS calculations<sup>3</sup> and  $0.270 \pm 0.001$  from RG calculations (field methods). These two theoretical values agree well with the experimental data; however, the average experimental value seems to be closer to the RG result.

#### E. Combination $R_{\xi}^+ R_c^{-1/3} = \xi_0^+(B^2/C^+)^{1/3}$

Combining  $R_{\xi}^+$  and  $R_c$  has the advantage of suppressing  $A^+$ , and a number of systems larger than for  $R_{\xi}^+$  or  $R_c$  can be considered. All the results are listed in Table V and compared in Fig. 5 to the theoretical values 0.650 (HTS)<sup>5</sup> and 0.667 (RG) which has been obtained using Refs. 3 and 5. The agreement is generally good. The low value found for the N-M system can be attributed to the inaccuracy of  $(\partial n / \partial \varphi)_{p,T}$ , which is due to the fact that the refractive indices of the components are nearly matched. This also leads to some uncertainty on the amplitude  $C^+$  deduced from turbidity measurements.

TABLE VI. Universal amplitude ratio  $R_{\xi}^+ = \xi_0^+(A^+)^{1/3}$ . Theoretical values are  $0.253 \pm 0.001$  (HTS), and  $0.270 \pm 0.001$  (RG).

| System | Measurements                  | $R_{\xi}^+$       |
|--------|-------------------------------|-------------------|
| A-C    | Refractive index <sup>b</sup> | $0.26 \pm 0.03$   |
| N-I    | Refractive index <sup>a</sup> | $0.298 \pm 0.034$ |
| T-W    | Calorimetry <sup>b</sup>      | $0.262 \pm 0.044$ |
|        | Density <sup>c</sup>          | $0.258 \pm 0.016$ |
| T-D    | Refractive index <sup>a</sup> | $0.260 \pm 0.029$ |
|        | Calorimetry <sup>b</sup>      | $0.250 \pm 0.027$ |
| I-W    | Calorimetry <sup>c</sup>      | $0.258 \pm 0.012$ |
|        | Density <sup>c,d</sup>        | $0.289 \pm 0.018$ |
|        | Volume <sup>c</sup>           | $0.319 \pm 0.030$ |
| N-M    | Refractive index <sup>a</sup> | $0.280 \pm 0.011$ |
|        | Density <sup>b,e</sup>        | $0.318 \pm 0.038$ |
| N-H    | Refractive index <sup>a</sup> | $0.27 \pm 0.03$   |
|        | Volume <sup>b</sup>           | $0.30 \pm 0.05$   |
| C-P    | Calorimetry <sup>c,d</sup>    | $0.248 \pm 0.026$ |
|        | Density <sup>c,d</sup>        | $0.248 \pm 0.032$ |

<sup>a</sup> $\xi_0$  and  $A^+$  from the same laboratory and measured in the same sample.

<sup>b</sup> $\xi_0$  and  $A^+$  measured in the same laboratory but not in the same sample.

<sup>c</sup> $\xi_0$  and  $A^+$  from different laboratories.

<sup>d</sup> $\alpha = 0.125$  in this case.

<sup>e</sup> $\alpha = 0.140$  in this case.

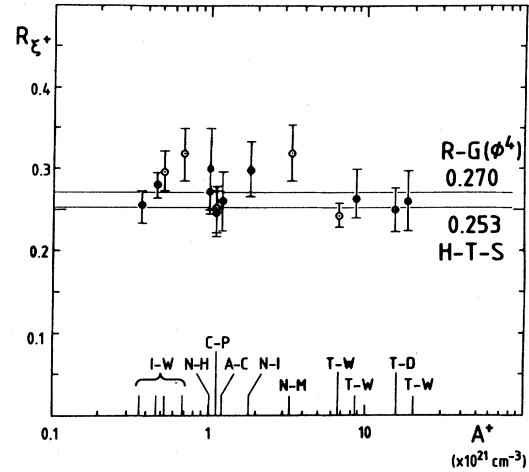


FIG. 4. Ratio  $R_{\xi}^+ = \xi_0^+(A^+)^{1/3}$  as a function of  $A^+$  for checking universality. Note the semilogarithmic scale. Eight systems have been studied. Full circles refer to refractive-index data, open circles to density measurements, and crosses to calorimetry determinations. Theoretical values are represented by full lines.

#### F. Combination $Q_2 = \frac{C^+}{C_c} \left( \frac{\xi_0^c}{\xi_0^+} \right)^{2-\eta}$

$Q_2$  has been measured in the system Nitrobenzene and *n*-Hexane<sup>21</sup>; the value found  $Q_2 = 1.1 \pm 0.3$  agrees well with the theoretical one, 1.21, obtained with the series method.<sup>4</sup>

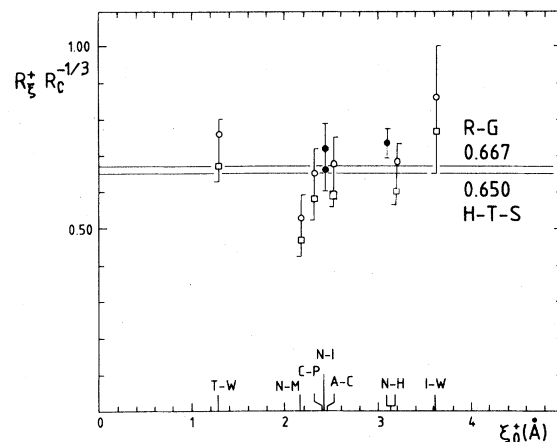


FIG. 5. Combination  $R_{\xi}^+ R_c^{-1/3} = \xi_0^+(B^2/C^+)^{1/3}$  as a function of  $\xi_0^+$  for testing universality. Seven systems are concerned. Full circles represent values obtained from the Rayleigh-Brillouin ratio, open circles concern the Yvon-Vuks theory, and open squares, the Rocard theory. Straight lines represent the theoretical values.

## VII. CONCLUSION

Each of the height amplitude ratios  $A^+/A^-$ ,  $\xi_0^+/\xi_0^-$ ,  $C^+/C^-$ ,  $R_c^+$ ,  $R_\chi^+$ ,  $R_\xi^+$ ,  $(R_\xi^+ R_c^{-1/3})$ , and  $Q_2$ , evaluated among eight different binary mixtures, are found to lie within a close range while some of the parameters which combine to enter in the ratios (such as the specific heat amplitude) vary by a large factor. This is well supported by the universality hypothesis of such ratios. Moreover, all experimental values are found to be in agreement with the theoretical values, especially for  $R_\xi^+$  which directly results from hyperscaling and whose determinations are in better accordance with the RG result than with the HTS calculation, known to violate hyperscaling. This result therefore agrees with the more recent calculations on critical exponents and their experimental determination in binary fluids.

Some problems, however, limit the possibilities of increasing the accuracy of such determinations. One is concerned with the difficulty of choosing the proper order parameter. An alternative was to consider the refractive index as a variable, but we are limited by the lack of knowledge concerning the variations—or the fluctuations (light scattering)—of the refractive index. More experimental and theoretical work is needed in this field. Another problem, still coupled to the refractive index, relates to the specific-heat amplitude obtained from refractive-index measurements. In all the systems which have been studied by this technique a good agreement is obtained when only the density dependence of the refractive index is taken into

account, suggesting that the fluctuation contribution is negligibly small. More work is necessary here also to definitely clarify this situation.

## APPENDIX A. TURBIDITY MEASUREMENTS

## 1. Experimental

The I-W mixture was prepared in a quartz cell (radius  $\approx 1$  cm, length  $= 2.000 \pm 0.001$  cm) and sealed at atmospheric pressure. The sample used was prepared with components from the same batch already used for the study reported in Ref. 46. Water comes from a highly sophisticated purification and filtration set up, the final quality corresponding to an Ohmic resistance of  $18 \text{ M}\Omega \text{ cm}$ . The purity of the acid was the best commercially available and exceeded 99%. The experimental mass fraction of the acid was  $0.3889 \pm 0.005$ , close to the critical mass fraction  $0.3885$  reported in Ref. 50.

The N-H system was prepared in a similar quartz cell. Since this system does not contain water, it was possible to freeze it at liquid nitrogen temperature and to seal it under a vacuum. Components were of spectroscopic grade and have been filtered through  $0.2\text{-}\mu\text{m}$  Teflon filters. The experimental mass fraction of nitrobenzene was  $0.509 \pm 0.002$ , the critical value being  $0.51$  according to Ref. 52 and  $0.525$  according to Ref. 21. This sample is the very same one which has been used already for the measurements of the Rayleigh-Brillouin ratio<sup>21</sup> and other determinations.<sup>53</sup>

The experimental set up is shown in Fig. 6. The

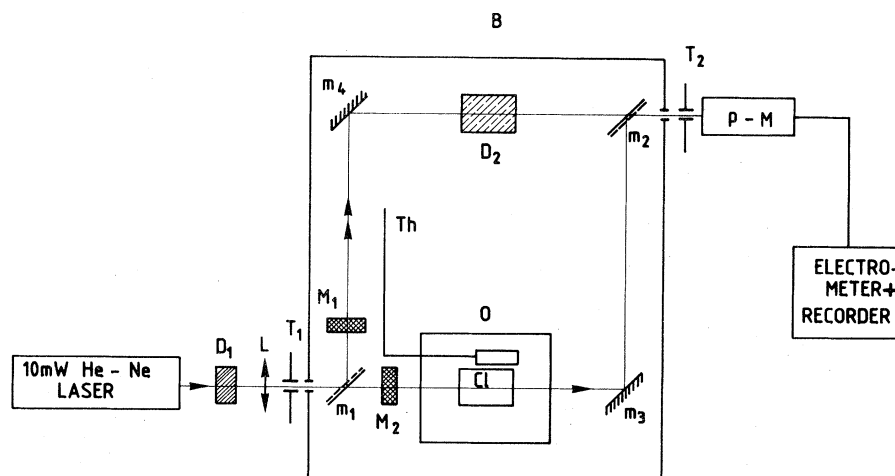


FIG. 6. Experimental set up used for turbidity measurements. Cl: cell; Th: quartz thermometer; O: copper oven with 0.1-mK stability; B: air regulated box with 20-mK stability;  $m_1$ ,  $m_2$ : semitransparent mirrors;  $m_3$ ,  $m_4$ : mirrors;  $M_1$ ,  $M_2$ : masks;  $D_1$ ,  $D_2$ : neutral densities; L: focusing lens;  $T_1$ ,  $T_2$ : pinholes.

sample was placed in a thermally stabilized copper oven giving a thermal stability of  $\pm 1 \times 10^{-4}$  over a period of several hours. This oven is enclosed in a thermally regulated box in which most of the optical arrangement is also set up. The principle is simple: the light beam from a He-Ne laser is first strongly attenuated by a neutral density filter to a few  $\mu\text{W}$ . This very low power cannot give spurious heating of the sample, whose temperature rise is typically 0.5 mK for 1-mW incident power. After the beam has been "cleaned" by a lens and a field stop, it is split into reference and measurement parts. Both are sent on a photomultiplier cathode, at the very same place, and the photocurrent is measured by an electrometer. Two masks allow either the optical balance to be performed or the transmitted beam to be measured. The linearity of the whole system was checked by varying the incident beam intensity by known amounts. A small pinhole was set just before the photomultiplier in order to reduce the aperture of collection, and then the scattering contributions. The overall relative accuracy was about 0.3%.

The critical temperature was assumed to be that corresponding to the lowest light transmission. This criterion is sometimes not sufficiently accurate since for a 2-cm length cell, the scattering contributions can prevent the transmission from canceling. In this case, we have taken advantage of the very intense and slowly varying speckles to improve the accuracy. These speckles indicate that the phase separation process is beginning. In this way, the critical temperature  $T_c$  can be obtained within 0.3 mK.

For each mixture, several sets of measurements have been made and no  $T_c$  drifts with time have been observed. Gravity effects are expected to be weak, since the beam diameter is small, and is located at the center of the sample where the concentration gradients vanish. Moreover, one of the mixture (I-W) has nearly matched component densities.

Data concerning the turbidity are listed in Table VII for the I-W system, and in Table VIII for the C-A system. Concerning this last mixture, the set up was somewhat different, and samples of various length have been used.<sup>30(b),54</sup> Data of the N-M system are listed in Ref. 32, and those of the C-P mixture are in Ref. 33.

## 2. Fitting procedure results

The turbidity measured at different temperatures, or composition<sup>21</sup>  $M$  using  $t = (M/B)^{1/\beta}$ , was

TABLE VII. Turbidity data for the system isobutyric acid + water.  $T_c = 27.0386^\circ\text{C}$ .

| $T - T_c$<br>( $\times 10^{-3}$ K) | Observations<br>( $\text{cm}^{-1}$ ) | $T - T_c$<br>( $\times 10^{-3}$ K) | Observations<br>( $\text{cm}^{-1}$ ) |
|------------------------------------|--------------------------------------|------------------------------------|--------------------------------------|
| First set                          |                                      |                                    |                                      |
| 1562.5                             | $5.700 \times 10^{-3}$               | 619.0                              | $2.909 \times 10^{-2}$               |
| 1343.7                             | $6.684 \times 10^{-3}$               | 380.3                              | $5.256 \times 10^{-2}$               |
| 1162.2                             | $9.296 \times 10^{-3}$               | 340.0                              | $5.788 \times 10^{-2}$               |
| 1020.7                             | $1.063 \times 10^{-2}$               | 460.1                              | $4.265 \times 10^{-2}$               |
| 911.9                              | $1.792 \times 10^{-2}$               | 570.7                              | $3.837 \times 10^{-2}$               |
| 802.3                              | $2.024 \times 10^{-2}$               | 319.7                              | $5.245 \times 10^{-2}$               |
| 802.1                              | $1.889 \times 10^{-2}$               | 299.0                              | $6.491 \times 10^{-2}$               |
| 576.8                              | $2.564 \times 10^{-2}$               | 278.7                              | $6.682 \times 10^{-2}$               |
| 461.1                              | $3.904 \times 10^{-2}$               | 263.8                              | $7.007 \times 10^{-2}$               |
| 366.9                              | $4.887 \times 10^{-2}$               | 202.4                              | $8.930 \times 10^{-2}$               |
| 215.3                              | $7.542 \times 10^{-2}$               | 140.1                              | $1.236 \times 10^{-1}$               |
| 192.2                              | $8.709 \times 10^{-2}$               | 98.3                               | $1.605 \times 10^{-1}$               |
| 167.7                              | $9.970 \times 10^{-2}$               | 77.1                               | $1.968 \times 10^{-1}$               |
| 143.2                              | $1.152 \times 10^{-1}$               | 55.8                               | $2.422 \times 10^{-1}$               |
| 118.5                              | $1.391 \times 10^{-1}$               | 45.4                               | $2.605 \times 10^{-1}$               |
| 93.9                               | $1.645 \times 10^{-1}$               | 34.1                               | $3.082 \times 10^{-1}$               |
| 69.0                               | $2.026 \times 10^{-1}$               | 23.5                               | $3.736 \times 10^{-1}$               |
| 44.5                               | $2.660 \times 10^{-1}$               | 18.2                               | $4.151 \times 10^{-1}$               |
| 32.1                               | $3.232 \times 10^{-1}$               | 9.9                                | $5.326 \times 10^{-1}$               |
| 26.9                               | $3.545 \times 10^{-1}$               | 13.9                               | $4.658 \times 10^{-1}$               |
| 126.3                              | $1.241 \times 10^{-1}$               | 7.7                                | $5.802 \times 10^{-1}$               |
| 96.7                               | $1.583 \times 10^{-1}$               | 5.6                                | $6.449 \times 10^{-1}$               |
| 74.4                               | $1.896 \times 10^{-1}$               | 3.5                                | $7.329 \times 10^{-1}$               |
| 49.4                               | $2.483 \times 10^{-1}$               | 2.4                                | $8.034 \times 10^{-1}$               |
| 36.9                               | $2.959 \times 10^{-1}$               | 1.4                                | $9.342 \times 10^{-1}$               |
| 21.6                               | $3.916 \times 10^{-1}$               |                                    |                                      |
| 16.6                               | $4.425 \times 10^{-1}$               |                                    |                                      |
| 14.2                               | $4.714 \times 10^{-1}$               |                                    |                                      |
| 11.6                               | $5.057 \times 10^{-1}$               |                                    |                                      |
| 10.4                               | $5.310 \times 10^{-1}$               |                                    |                                      |
| 9.2                                | $5.538 \times 10^{-1}$               |                                    |                                      |
| 8.0                                | $5.792 \times 10^{-1}$               |                                    |                                      |
| 6.8                                | $6.152 \times 10^{-1}$               |                                    |                                      |
| 6.3                                | $6.282 \times 10^{-1}$               |                                    |                                      |
| 5.9                                | $6.462 \times 10^{-1}$               |                                    |                                      |
| 5.2                                | $6.636 \times 10^{-1}$               |                                    |                                      |
| 4.8                                | $6.846 \times 10^{-1}$               |                                    |                                      |
| 3.8                                | $7.341 \times 10^{-1}$               |                                    |                                      |
| Second set                         |                                      |                                    |                                      |
| 1336.0                             | $1.395 \times 10^{-2}$               |                                    |                                      |
| 858.0                              | $2.246 \times 10^{-2}$               |                                    |                                      |

fitted to the following expression, deduced from the relations (13)–(16):

$$\tau + \alpha_0 = \tau_0(1+t)t^{-\gamma}G'(\sqrt{2}K_0\xi_0t^{-\nu}) + \alpha_0, \quad (\text{A1})$$

where the quantities  $\gamma$  and  $\nu$ , and  $\tau_0$ ,  $\xi_0$ , and  $\alpha_0$

TABLE VIII. Turbidity data of the system cyclohexane + aniline.  $T_c = 30.15^\circ\text{C}$ . For absolute values, multiply the observations by 2.30.

| $T - T_c (\times 10^{-3} \text{ K})$ | Observations<br>( $\text{cm}^{-1}$ ) | $T - T_c (\times 10^{-3} \text{ K})$ | Observations<br>( $\text{cm}^{-1}$ ) | $T - T_c (\times 10^{-3} \text{ K})$ | Observations<br>( $\text{cm}^{-1}$ ) |
|--------------------------------------|--------------------------------------|--------------------------------------|--------------------------------------|--------------------------------------|--------------------------------------|
| 1.0                                  | $2.00 \times 10^0$                   | 78.3                                 | $2.87 \times 10^{-1}$                | 370.3                                | $7.80 \times 10^{-2}$                |
| 3.0                                  | $1.61 \times 10^0$                   | 81.0                                 | $2.92 \times 10^{-1}$                | 385.5                                | $6.80 \times 10^{-1}$                |
| 7.0                                  | $1.13 \times 10^0$                   | 92.8                                 | $2.39 \times 10^{-1}$                | 475.6                                | $5.40 \times 10^{-2}$                |
| 9.9                                  | $9.88 \times 10^{-1}$                | 93.1                                 | $2.51 \times 10^{-1}$                | 520.5                                | $5.20 \times 10^{-2}$                |
| 11.8                                 | $9.54 \times 10^{-1}$                | 93.0                                 | $2.51 \times 10^{-1}$                | 630.6                                | $3.95 \times 10^{-2}$                |
| 12.2                                 | $9.00 \times 10^{-1}$                | 100.0                                | $2.28 \times 10^{-1}$                | 665.8                                | $3.90 \times 10^{-2}$                |
| 13.0                                 | $8.76 \times 10^{-1}$                | 102.0                                | $2.25 \times 10^{-1}$                | 760.7                                | $3.30 \times 10^{-2}$                |
| 14.0                                 | $8.60 \times 10^{-1}$                | 108.0                                | $2.26 \times 10^{-1}$                | 849.2                                | $2.70 \times 10^{-2}$                |
| 15.8                                 | $8.05 \times 10^{-1}$                | 111.0                                | $2.17 \times 10^{-1}$                | 849.2                                | $2.53 \times 10^{-2}$                |
| 16.1                                 | $8.54 \times 10^{-1}$                | 118.0                                | $2.26 \times 10^{-1}$                | 921.1                                | $2.67 \times 10^{-2}$                |
| 16.7                                 | $7.65 \times 10^{-1}$                | 118.0                                | $2.16 \times 10^{-1}$                | 919.0                                | $2.20 \times 10^{-2}$                |
| 19.1                                 | $7.23 \times 10^{-1}$                | 118.9                                | $1.97 \times 10^{-1}$                | 1000.9                               | $1.85 \times 10^{-2}$                |
| 20.0                                 | $7.55 \times 10^{-1}$                | 121.0                                | $2.04 \times 10^{-1}$                | 1161.0                               | $1.52 \times 10^{-2}$                |
| 22.0                                 | $7.00 \times 10^{-1}$                | 131.0                                | $1.91 \times 10^{-1}$                | 1264.8                               | $1.37 \times 10^{-2}$                |
| 23.0                                 | $6.99 \times 10^{-1}$                | 136.8                                | $1.77 \times 10^{-1}$                | 1528.6                               | $1.27 \times 10^{-2}$                |
| 23.0                                 | $6.90 \times 10^{-1}$                | 142.0                                | $1.86 \times 10^{-1}$                | 1674.2                               | $1.23 \times 10^{-2}$                |
| 24.3                                 | $6.38 \times 10^{-1}$                | 145.0                                | $1.70 \times 10^{-1}$                | 1789.5                               | $1.12 \times 10^{-2}$                |
| 24.9                                 | $6.21 \times 10^{-1}$                | 145.0                                | $1.64 \times 10^{-1}$                | 1913.8                               | $1.02 \times 10^{-2}$                |
| 26.1                                 | $6.37 \times 10^{-1}$                | 153.8                                | $1.62 \times 10^{-1}$                | 2001.8                               | $9.70 \times 10^{-3}$                |
| 28.8                                 | $5.83 \times 10^{-1}$                | 154.0                                | $1.67 \times 10^{-1}$                | 2368.8                               | $8.80 \times 10^{-3}$                |
| 28.9                                 | $5.71 \times 10^{-1}$                | 156.2                                | $1.50 \times 10^{-1}$                | 2647.8                               | $7.60 \times 10^{-3}$                |
| 32.8                                 | $5.42 \times 10^{-1}$                | 162.0                                | $1.61 \times 10^{-1}$                | 3124.0                               | $5.90 \times 10^{-3}$                |
| 33.0                                 | $5.43 \times 10^{-1}$                | 162.9                                | $1.66 \times 10^{-1}$                | 3163.4                               | $4.20 \times 10^{-3}$                |
| 34.9                                 | $5.11 \times 10^{-1}$                | 167.1                                | $1.44 \times 10^{-1}$                | 3852.0                               | $4.80 \times 10^{-3}$                |
| 34.9                                 | $5.08 \times 10^{-1}$                | 180.0                                | $1.40 \times 10^{-1}$                |                                      |                                      |
| 37.9                                 | $4.90 \times 10^{-1}$                | 180.5                                | $1.35 \times 10^{-1}$                |                                      |                                      |
| 40.0                                 | $4.82 \times 10^{-1}$                | 186.0                                | $1.31 \times 10^{-1}$                |                                      |                                      |
| 40.0                                 | $4.89 \times 10^{-1}$                | 196.0                                | $1.44 \times 10^{-1}$                |                                      |                                      |
| 41.2                                 | $4.49 \times 10^{-1}$                | 199.0                                | $1.24 \times 10^{-1}$                |                                      |                                      |
| 43.1                                 | $4.59 \times 10^{-1}$                | 200.0                                | $1.25 \times 10^{-1}$                |                                      |                                      |
| 44.0                                 | $4.37 \times 10^{-1}$                | 206.0                                | $1.16 \times 10^{-1}$                |                                      |                                      |
| 45.8                                 | $4.26 \times 10^{-1}$                | 207.2                                | $1.31 \times 10^{-1}$                |                                      |                                      |
| 51.0                                 | $4.10 \times 10^{-1}$                | 242.3                                | $1.11 \times 10^{-1}$                |                                      |                                      |
| 54.6                                 | $3.73 \times 10^{-1}$                | 245.0                                | $1.05 \times 10^{-1}$                |                                      |                                      |
| 55.2                                 | $3.74 \times 10^{-1}$                | 248.7                                | $1.04 \times 10^{-1}$                |                                      |                                      |
| 59.5                                 | $3.46 \times 10^{-1}$                | 251.1                                | $1.11 \times 10^{-1}$                |                                      |                                      |
| 60.1                                 | $3.68 \times 10^{-1}$                | 252.0                                | $1.12 \times 10^{-1}$                |                                      |                                      |
| 62.8                                 | $3.40 \times 10^{-1}$                | 262.7                                | $8.80 \times 10^{-2}$                |                                      |                                      |
| 64.0                                 | $3.41 \times 10^{-1}$                | 271.1                                | $9.50 \times 10^{-2}$                |                                      |                                      |
| 64.9                                 | $3.37 \times 10^{-1}$                | 283.9                                | $1.09 \times 10^{-1}$                |                                      |                                      |
| 71.3                                 | $3.10 \times 10^{-1}$                | 299.0                                | $9.70 \times 10^{-2}$                |                                      |                                      |
| 72.5                                 | $3.00 \times 10^{-1}$                | 326.0                                | $8.00 \times 10^{-2}$                |                                      |                                      |
| 74.0                                 | $3.05 \times 10^{-1}$                | 328.8                                | $8.20 \times 10^{-2}$                |                                      |                                      |
| 75.2                                 | $2.92 \times 10^{-1}$                | 331.2                                | $8.00 \times 10^{-2}$                |                                      |                                      |
| 77.0                                 | $2.84 \times 10^{-1}$                | 360.3                                | $7.00 \times 10^{-2}$                |                                      |                                      |

have been regarded as adjustable parameters; the exponent  $\eta$  in  $G'$  was supposed to be 0.0315. A first fit was made to check the values of the exponents  $\gamma$  and  $\nu$ , excepted for the N-M system

which is weakly turbid and gives results with poor accuracy. Then a second fit was made with  $\gamma$  and  $\nu$  having their theoretical values 1.240 and 0.630; this leads to smaller uncertainties for the ampli-



TABLE IX. Critical exponents and amplitudes deduced from turbidity measurements. Data are fitted to formula (A1).

| System           | Parameters            | $\gamma$          | $\nu$             | $\xi_0$ (Å)       | $\tau_0(10^{-5} \text{ cm}^{-1})$ | $Q$   |
|------------------|-----------------------|-------------------|-------------------|-------------------|-----------------------------------|-------|
| A-C              | All free              | $1.250 \pm 0.076$ | $0.626 \pm 0.028$ | $2.68 \pm 0.31$   | $3.0 \pm 1.5$                     | 0.863 |
|                  | $\gamma, \nu$ imposed | (1.240)           | (0.630)           | $2.45 \pm 0.05$   | $3.05 \pm 0.06$                   | 0.804 |
| I-W              | All free              | $1.24 \pm 0.10$   | $0.631 \pm 0.045$ | $3.6 \pm 0.8$     | $1.1 \pm 0.8$                     | 0.453 |
|                  | $\gamma, \nu$ imposed | (1.240)           | (0.630)           | $3.625 \pm 0.065$ | $1.08 \pm 0.02$                   | 0.454 |
| N-M <sup>a</sup> | $\gamma, \nu$ imposed | (1.240)           | (0.630)           | $2.36 \pm 0.30$   | $0.027 \pm 0.006$                 | 0.752 |
| C-P <sup>b</sup> | All free              | $1.29 \pm 0.18$   | $0.62 \pm 0.09$   | $2.4 \pm 3$       | $1.7 \pm 1.8$                     | 0.825 |
|                  | $\gamma, \nu$ imposed | (1.240)           | (0.630)           | $2.40 \pm 0.20$   | $2.69 \pm 0.15$                   | 0.472 |

<sup>a</sup>Data from Ref. 32.

<sup>b</sup>Data from Ref. 33.

tudes  $\tau_0$  and  $\xi_0$ . The results are reported in Table IX, and the deviations to the most significant fit are shown in Fig. 7.

The I-W, T-W, and N-M systems are not very turbid, and the scattering contributions near  $T_c$  remain negligible. No data very close to  $T_c$  have been reported for the C-P mixture. The use of thin samples of C-A have made the contribution of

scattering negligible, and has allowed accurate measurements to be made near  $T_c$ . This was not the case for the N-H system, which is highly turbid; the data, their analysis, and a complete discussion for this particular system can be found in Ref. 21.

The fitting procedure that we used is non-linear.<sup>55</sup> The data statistical quality of the fit is measured by the coefficient  $Q$ , which is equal to one only when the deviations are purely random. The uncertainty on the parameters corresponds to about two standard deviations of a least-squares fit.

#### APPENDIX B: SPECIFIC-HEAT-DATA ANALYSIS (I-W)

The specific-heat data from Ref. 56 which concern the I-W mixture in the homogeneous region  $T > T_c$ , have been fitted to the formula (4) where the corrections to scaling have been found to be negligible, i.e.,

$$C_{p,i}/k_B = A^+/\alpha + C_R^+ . \quad (\text{B1})$$

$A^+$  and  $C_R^+$  were the adjustable parameters, and  $\alpha$  was fixed to its theoretical value  $\alpha = 0.110$ . The following numerical values were found:  $A^+ = (0.362 \pm 0.015) \times 10^{21}$  and  $C_R^+ = (2.4 \pm 0.4) 10^{23} \text{ cm}^{-3}$ . The statistical quality of the fit was very good (factor of  $Q = 0.936$ ).

#### APPENDIX C: DENSITY-DATA ANALYSIS (T-W)

The density of the T-W mixture, from Ref. 57, has been fitted to the following function, directly deduced from the formulas (4) and (18):

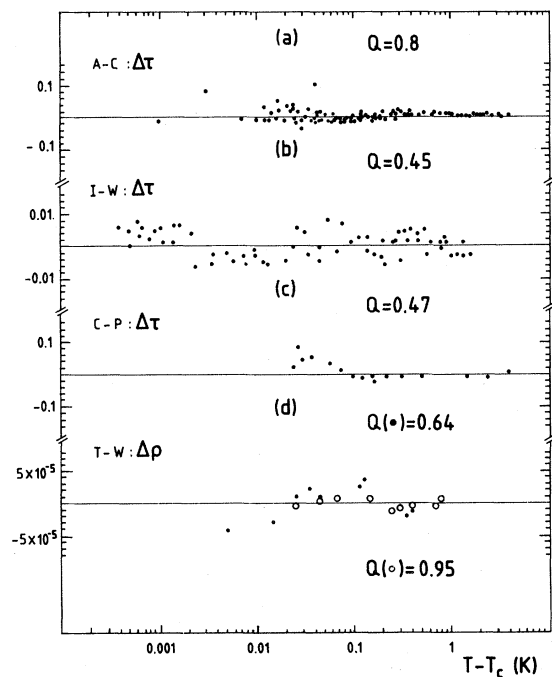


FIG. 7. (a), (b), and (c) Deviation  $\Delta\tau$  between the experimental values of the turbidity and the "best" calculated values reported in Table IX. (d) Deviation  $\Delta\rho$  between the density data of the triethylamine + water system and the best fits of Table X. Full circles correspond to the inhomogeneous region  $T > T_c$ , open circles to the homogeneous one  $T < T_c$ .

TABLE X. Fit of the T-W density data from Ref. 56 to formula (C1).

| T-W       |                     | $\rho_1$  | $\rho_2$                             | $Q$            |
|-----------|---------------------|---|--------------------------------------|----------------|
| $T < T_c$ | Without corrections | $0.015 \pm 0.015$<br>( $0.15 \pm 0.02$ )<br>imposed   | $0.26 \pm 0.01$<br>$0.19 \pm 0.01$   | 0.503<br>0.759 |
|           | homogeneous (+)     | With corrections<br>$\alpha a_c^+ = -4.45$<br>imposed | $0.21 \pm 0.05$<br>$0.233 \pm 0.013$ | 0.770<br>0.954 |
| $T > T_c$ | Without corrections | $0.73 \pm 0.22$<br>( $0.16 \pm 0.02$ )<br>imposed     | $0.3 \pm 0.1$<br>$0.537 \pm 0.011$   | 0.814<br>0.750 |
|           | inhomogeneous (-)   | With corrections<br>$\alpha a_c^- = -4.45$<br>imposed | $0.87 \pm 0.13$<br>$0.640 \pm 0.016$ | 0.850<br>0.639 |

$$\rho^\pm = \rho_c \pm \rho_1^\pm t \pm \rho_2^\pm t^{1-\alpha} (1 + \alpha a_c^\pm t^\Delta). \quad (\text{C1})$$

The coefficient  $\rho_1^\pm$  can be related to the regular thermal expansion coefficient

$$\text{reg} \alpha_{p,i}^\pm = \rho_1^\pm (\rho_c T_c), \quad (\text{C2})$$

and  $\rho_2^\pm$  to the amplitude of the specific heat  $A^\pm$  by

$$A^\pm = \frac{\alpha(1-\alpha)}{k_B \left[ \frac{dT_c}{dp} \right]_{v,i}} \rho_2^\pm. \quad (\text{C3})$$

Because of the small  $t$  range investigated, the exponents have been always imposed to their theoretical values  $\alpha=0.110$  and  $\Delta=0.50$ , and the correction-to-scaling amplitude has been either set to zero or imposed to the value  $\alpha a_c^+ = -4.45$  found in Ref. 46 and assessed in Ref. 16. From a theoretical point of view,  $a_c^+$  is expected to be equal to  $a_c^-$ . Also the regular contribution has been estimated, within 13%, at the ideal value. In Table X are reported the results of such a fit. It is interesting to note that the introduction of corrections modifies the amplitude values and, in the region (+), increases the statistical quality of the fit, measured by  $Q$ . See also Fig. 7(d) where the deviations are plotted.

We think that the more reliable values are those obtained with the correction-to-scaling terms and with the regular contribution estimated; these values have been reported in Table III.

TABLE XI. Thermal derivative of the refractive index:  $(\partial n / \partial T)_{p,i}$  in the aniline-cyclohexane system.  $T_c = 29.50$  °C, from Ref. 34. Accuracy on  $(\partial n / \partial T)_{p,i}$  is about  $8 \times 10^{-6}$ .

| $T - T_c$ | $\left[ \frac{\partial n}{\partial T} \right]_{p,i}$<br>( $\times 10^{-4} \text{ K}^{-1}$ ) |
|-----------|---|
| 13.5      | 5.308   |
| 9.5       | 5.498   |
| 8.7       | 5.393   |
| 8.5       | 5.260   |
| 8.2       | 5.498   |
| 8.0       | 5.507   |
| 7.8       | 5.545   |
| 7.5       | 5.440   |
| 7.0       | 5.498   |
| 6.5       | 5.531   |
| 6.0       | 5.450   |
| 5.7       | 5.521   |
| 5.0       | 5.498   |
| 4.8       | 5.507   |
| 4.3       | 5.440   |
| 3.8       | 5.474   |
| 3.4       | 5.640   |
| 2.8       | 5.474   |
| 2.6       | 5.640   |
| 2.3       | 5.426   |
| 1.9       | 5.521   |
| 1.8       | 5.640   |
| 1.3       | 5.640   |
| 0.8       | 5.593   |
| 0.3       | 5.735   |

APPENDIX D: REFRACTIVE-INDEX  
DATA ANALYSIS (C-A, N-I)

The data on the C-A system come from Ref. 34, and have been listed in Table XI. Only the slope  $(\partial n/\partial T)_{p,i}$  is available, in a range  $t = 10^{-3} - 0.05$ . Indeed the high turbidity of this system prevents accurate determinations to be made close to  $T_c$ . These data were compared to the derivative of formula (22):

$$\left(\frac{\partial n}{\partial T}\right)_{p,i} = \left(\frac{\partial n}{\partial T}\right)_{p,i}^{\text{reg}} + \left(\frac{1-\alpha}{T_c}\right) R t^{-\alpha}, \quad (\text{D1})$$

with  $(\partial n/\partial T)_{p,i}^{\text{reg}}$  and  $R$  as adjustable parameters.  $T_c$  was set to 303 K (Table XII), and  $\alpha$  to the theoretical value 0.110. In order to improve the accuracy of the results, we have estimated the ideal value  $(\partial n/\partial T)_{p,i}^{\text{id}}$  assuming volume additivity. Using  $(\partial n/\partial T)_p^A = -(5.1 \pm 0.1)10^{-4} \text{ K}^{-1}$  from Ref. 58 (the uncertainty has been estimated by us) for aniline and  $(\partial n/\partial T)_p^C = -(5.561 \pm 0.006)10^{-4} \text{ K}^{-1}$  from Ref. 47 for cyclohexane, we get  $(\partial n/\partial T)_{p,i}^{\text{id}} = -(5.30 \pm 0.08)10^{-4} \text{ K}^{-1}$ . Only when the regular part was estimated at this value was a significant accuracy obtained for  $R$ . In fact  $(\partial n/\partial T)_{p,i}^{\text{reg}}$  was not strictly fixed, as shown in Table XII, where the obtained value is slightly different from the starting value, and where the accuracy is increased. The experimental data have influenced the final results, but with a statistical weighting smaller than the starting value of  $(\partial n/\partial T)_{p,i}^{\text{reg}}$ . The statistical quality of the fit is very good, as shown by the  $Q$  value which is nearly equal to one.

We have also reanalyzed the refractive index data of Ref. 49, obtained in the two-phase region of the N-I system. With  $u(l)$  denoting the upper (lower) phase, and with

$$c^{u,l} = c_c + B t^\beta \quad (\text{D2})$$

the mass fraction of one component, one easily obtains, according to the Lorentz-Lorenz formula, and the fact that the refractive index of the components are closely matched,

$$n^{u,l} - n_c = T_c \left(\frac{\partial n}{\partial T}\right)_{p,c}^{\text{reg}} t - R^- |t|^{1-\alpha} + \left(\frac{\partial n}{\partial c}\right)_{p,T} B |t|^\beta. \quad (\text{D3})$$

$+$  ( $-$ ) refers to the  $u(l)$  phase. The fit whose results are shown in Table XII has been performed with  $n_c$ ,  $R^-$ ,  $[(\partial n/\partial c)_{p,T} B]$  free, and  $\alpha (=0.110)$  and  $\beta (=0.325)$  imposed. Following the arguments developed in Ref. 40, the value of  $(\partial n/\partial T)_{p,c}^{\text{reg}}$  has been imposed within the known uncertainties. When one compares the  $R^-$  value with  $R^+$  from Ref. 40, correcting for the different definitions of  $R$ , one finds  $R^+/R^- = 0.56 \pm 0.09$ , a value reported in Table III. Note that the value of  $[(\partial n/\partial c)_{p,T} B]$  which is found here is in full agreement with that reported in Ref. 49.

APPENDIX E: COEXISTENCE-CURVE  
ANALYSIS (C-A, N-M, N-H, AND C-P)

All data have been reduced in volume fraction  $\varphi$ , assuming volume additivity. However this assumption may fail for systems with strong nonideality, which are not considered here. The relationship

$$\varphi_1^{-1} = 1 - \beta_0 + \beta_0 c_1^{-1} \quad (\text{E1})$$

has been used, with  $c_1$ , the mass fraction of component 1 and  $\beta_0 = \rho_1/\rho_2$  the ratio of mass densities

TABLE XII. Fit of the formula (D1) to A-C data  $(\partial n/\partial T)_{p,i}$ , and of the formula (D3) to N-I data ( $n$ ).

| System<br>( $\lambda = 6328 \text{ \AA}$ ) | $(\partial n/\partial T)_{p,i}^{\text{reg}}$<br>( $\times 10^{-4} \text{ K}^{-1}$ ) | $R$<br>( $\times 10^{-2}$ ) | $\alpha$ | $[(\partial u/\partial c)_{p,T} B]$<br>( $\times 10^{-4}$ ) | $Q$   |
|--|---|-----------------------------|----------|---|-------|
| A-C <sup>a</sup>                           | $(-5.17 \pm 0.07)$  | $-0.7 \pm 0.2$              | (0.110)  |   | 0.960 |
| (+) region                                 | imposed   |                             | imposed  |   |       |
| N-I <sup>b</sup>                           | $(-4.779 \pm 0.010)$  | $-0.513 \pm 0.052$          | (0.110)  | $12.1 \pm 0.4$  | 0.599 |
| (-) region                                 | imposed   |                             | imposed  |   |       |

<sup>a</sup>Data from Table XI.

<sup>b</sup>Data from Ref. 49.

TABLE XIII. Determination of the coexistence curve parameters (Eq. E3).

| System | measurement          | $\varphi_c$<br>(First component) | $T_c$  | $B_\varphi$       | $a_m$         | $E$               | $\beta'$  | $Q$             |                 |               |       |
|--------|----------------------|----------------------------------|--|-------------------|---------------|-------------------|---|-----------------|-----------------|---------------|-------|
| A-C    | Density <sup>a</sup> | $0.3610 \pm 0.0012$              | $\left[ \begin{array}{c} 29.915 \\ \text{imposed} \end{array} \right]$ | $0.97 \pm 0.03$   | $0.9 \pm 0.4$ |                   |   | 0.529           |                 |               |       |
|        |                      | $0.3610 \pm 0.0015$              |  | $1.03 \pm 0.03$   |               |                   |   | 0.532           |                 |               |       |
| N-M    | Density <sup>b</sup> | $0.3575 \pm 0.0040$              | $\left[ \begin{array}{c} 26.472 \\ \text{imposed} \end{array} \right]$ | $0.852 \pm 0.005$ | $0.3 \pm 0.1$ | $0.25 \pm 0.02$   | $\left[ \begin{array}{c} 0.650 \\ \text{imposed} \end{array} \right]$ | 0.593           |                 |               |       |
|        |                      | $0.356 \pm 0.001$                |  | $0.852 \pm 0.001$ |               |                   |   | $0.3 \pm 0.1$   | $0.10 \pm 0.05$ | $0.5 \pm 0.1$ | 0.625 |
|        |                      | $0.356 \pm 0.001$                |  | $0.865 \pm 0.001$ |               |                   |   |                 | $0.10 \pm 0.5$  | $0.5 \pm 0.1$ | 0.547 |
| N-H    | Visual <sup>c</sup>  | $0.370 \pm 0.003$                | $19.01 \pm 0.06$   | $0.770 \pm 0.006$ |               | $0.258 \pm 0.003$ | $\left[ \begin{array}{c} 0.650 \\ \text{imposed} \end{array} \right]$ | 0.274           |                 |               |       |
|        |                      | $0.37 \pm 0.01$                  | $19.02 \pm 0.09$   | $0.770 \pm 0.008$ |               |                   |   | $0.28 \pm 0.26$ | $0.7 \pm 0.4$   | 0.259         |       |
|        |                      | $0.377 \pm 0.003$                | $19.06 \pm 0.07$   | $0.767 \pm 0.007$ |               |                   |   | $0.61 \pm 0.08$ | (1 imposed)     | 0.230         |       |
| C-P    | Visual <sup>d</sup>  | $0.5525 \pm 0.0003$              | $28.4710 \pm 0.0006$   | $0.844 \pm 0.013$ | $1.6 \pm 0.6$ |                   |   | 0.949           |                 |               |       |
|        |                      | $0.504 \pm 0.030$                | $28.4720 \pm 0.0006$   | $0.85 \pm 0.01$   | $1.2 \pm 0.6$ | $0.05 \pm 0.03$   | $0.010 \pm 0.003$   |                 | 0.762           |               |       |

<sup>a</sup>Reference 69.<sup>b</sup>Reference 70.<sup>c</sup>Reference 61.<sup>d</sup>Reference 37.

of pure components 1 and 2. When the mass density  $\rho_1^{u,l}$  of component 1 in the upper (lower) phase is known, one can deduce  $\varphi$  from

$$\varphi^{u,l} = (\rho_1^{u,l} - \rho_2) / (\rho_1 - \rho_2). \quad (\text{E2})$$

The thermal variations of  $\rho_1, \rho_2$  have been accounted for. The data have been fitted to

$$\varphi^{u,l} = \varphi_c \pm B_\varphi t^\beta (1 + \alpha_m t^\Delta) + E t^{\beta'}, \quad (\text{E3})$$

where  $\beta = 0.325$  and  $\Delta = 0.50$  were imposed. The parameters  $\varphi_c, T_c$  which appear in

$t = |(T - T_c)/T_c|$ ,  $B_\varphi, a_m$ , and  $E$  are free.  $\beta'$  is either free, or imposed to 1 or  $2\beta = 0.65$  when a first fit shows that  $E$  is different from zero. All results are given in Table XIII. One can notice that for all systems the value of the amplitude  $B_\varphi$  does not vary very much according to the different assumptions. Corrections to scaling have been found somewhat significant only in the C-P system. We have considered as more probable the determinations performed in the first line for each system, and reported the corresponding amplitudes in Table IV.

<sup>1</sup>For review, see *Phase Transitions, Status of the Experimental and Theoretical Situation, Cargese, 1980*, edited by M. Levy, J. C. Le Guillou, and J. Zinn-Justin (Plenum, New York, 1981).

<sup>2</sup>P. Scheffeld, J. D. Litster, and J. T. Ho, *Phys. Rev. Lett.* **23**, 1098 (1969).

<sup>3</sup>D. Stauffer, M. Ferer, and M. Wortis, *Phys. Rev. Lett.* **29**, 345 (1972).

<sup>4</sup>E. Brezin, J. C. LeGuillou, and J. Zinn-Justin, *Phys. Lett.* **47A**, 285 (1974) and in *Phase Transitions and Critical Phenomena*, edited by C. Domb and M. S. Green (Academic, New York, 1976).

<sup>5</sup>P. C. Hohenberg, A. Aharony, B. I. Halperin, and E. D. Siggia, *Phys. Rev. B* **13**, 2986 (1976).

<sup>6</sup>C. Bervillier, *Phys. Rev. B* **14**, 4964 (1976).

<sup>7</sup>C. Bervillier, and C. Godreche, *Phys. Rev. B* **21**, 5427 (1980).

<sup>8</sup>H. Klein and D. Woermann, *J. Chem. Phys.* **64**, 5316 (1976); **65**, 1599 (1976).

<sup>9</sup>J. V. Sengers and M. R. Moldover, *Phys. Lett.* **66A**, 44 (1978).

<sup>10</sup>D. Beysens, R. Tufeu, and Y. Garrabos, *J. Phys. Lett. (Paris)* **40**, L-623 (1979).

<sup>11</sup>D. Beysens, in Ref. 1.

<sup>12</sup>J. V. Sengers, in Ref. 1.

<sup>13</sup>M. C. Chang and A. Houghton, *Phys. Rev. Lett.* **44**, 785 (1980).

<sup>14</sup>A. Aharony and G. Ahlers, *Phys. Rev. Lett.* **44**, 782

- (1980).
- <sup>15</sup>C. Bagnuls and C. Bervillier, *Phys. Rev. B* **24**, 1226 (1981).
- <sup>16</sup>A. Bourgou and D. Beysens, *Phys. Rev. Lett.* **47**, 257 (1981).
- <sup>17</sup>J. C. Le Guillou and J. Zinn-Justin, *Phys. Rev. Lett.* **39**, 95 (1977); *Phys. Rev. B* **21**, 3976 (1980).
- <sup>18</sup>B. G. Nickel, in Ref. 1
- <sup>19</sup>J. Zinn-Justin, *J. Phys. (Paris)* **42**, 783 (1981).
- <sup>20</sup>M. Ley-Koo and M. S. Green, *Phys. Rev. A* **23**, 2650 (1981).
- <sup>21</sup>G. Zalczer, A. Bourgou, and D. Beysens, (Saclay report No. SRM/82/2000, 1982) (unpublished).
- <sup>22</sup>See for instance, B. J. Berne and P. Pecora, *Dynamic Light Scattering* (Wiley, New York, 1976).
- <sup>23</sup>A. J. Bray, *Phys. Rev. B* **14**, 1248 (1976), and references therein.
- <sup>24</sup>R. F. Chang, H. Burstyn, J. V. Sengers, and A. J. Bray, *Phys. Rev. A* **19**, 866 (1979).
- <sup>25</sup>M. E. Fisher and J. S. Langer, *Phys. Rev. Lett.* **20**, 665 (1968).
- <sup>26</sup>Y. Garrabos, G. Zalczer, and D. Beysens, *Phys. Rev. A* **25**, 1147 (1982).
- <sup>27</sup>N. B. Rozhdestvenskaya and E. N. Gorbschova, *Opt. Commun.* **30**, 383 (1979).
- <sup>28</sup>M. F. Vuks, *Opt. Spectrosc.* **28**, 71 (1970).
- <sup>29</sup>D. Beysens, *J. Chem. Phys.* **64**, 2579 (1976).
- <sup>30</sup>(a) Y. Garrabos, R. Tufeu, and B. Le Neindre, *J. Chem. Phys.* **68**, 495 (1978); (b) P. Calmettes, I. Lagues, and C. Laj, *Phys. Rev. Lett.* **28**, 478 (1972).
- <sup>31</sup>D. Beysens and A. Bourgou (unpublished).
- <sup>32</sup>H. Burstyn, PhD. thesis, University of Maryland, 1979 (unpublished).
- <sup>33</sup>D. Thiel, B. Chu, A. Stein, and G. Allen, *J. Chem. Phys.* **62**, 3689 (1975).
- <sup>34</sup>P. Calmettes, Saclay Report No. DPh-T/SRM/78/1545, 1978 (unpublished).
- <sup>35</sup>E. Bloemen, J. Thoen, and W. Van Daël, *J. Chem. Phys.* **73**, 4628 (1980).
- <sup>36</sup>See, for instance, M. A. Anisimov, A. V. Voronel, and T. M. Ovodona, *Zh. Eksp. Teor. Fiz.* **61**, 1092 (1971) [*Sov. Phys. JETP* **34**, 583 (1972)].
- <sup>37</sup>P. Pelger, H. Klein, and D. Woermann, *J. Chem. Phys.* **67**, 5362 (1977).
- <sup>38</sup>J. Thoen, E. Bloemen, and W. Van Daël, *J. Chem. Phys.* **68**, 735 (1978).
- <sup>39</sup>See, for instance, D. Beysens, M. Gbadamassi, and L. Boyer, *Phys. Rev. Lett.* **43**, 1253 (1979); D. Beysens and M. Gbadamassi, *Phys. Rev. A* **22**, 2250 (1980) and references therein.
- <sup>40</sup>D. Beysens and J. Weisfred, *J. Chem. Phys.* **71**, 119 (1979).
- <sup>41</sup>D. Beysens and A. Bourgou, in the Proceedings of the International Joint Conference on Thermophysical Properties, Gaithersburg, 1981 (in press).
- <sup>42</sup>J. V. Sengers, D. Bedeaux, P. Mazur, and S. C. Green, *Physica (Utrecht)* **A104**, 573 (1980).
- <sup>43</sup>G. Stell and J. S. Høye, *Phys. Rev. Lett.* **33**, 1268 (1974).
- <sup>44</sup>D. Beysens and M. Gbadamassi, *Phys. Rev. Lett.* **47**, 846 (1981); Y. C. Chou and W. I. Goldberg, *ibid.* **47**, 1155 (1981).
- <sup>45</sup>A. Onuki and K. Kawasaki, *Phys. Lett.* **78A**, 354 (1980).
- <sup>46</sup>D. Beysens and A. Bourgou, *Phys. Rev. A* **19**, 2407 (1979).
- <sup>47</sup>D. Beysens and P. Calmettes, *J. Chem. Phys.* **66**, 766 (1977).
- <sup>48</sup>J. Sengers, in Ref. 1.
- <sup>49</sup>D. Beysens, *J. Chem. Phys.* **71**, 2557 (1979).
- <sup>50</sup>S. C. Greer, *Phys. Rev. A* **14**, 1770 (1976).
- <sup>51</sup>D. A. Balzarini, *Can. J. Phys.* **52**, 499 (1974).
- <sup>52</sup>S. H. Chen and N. Polonsky, *Phys. Rev. Lett.* **20**, 909 (1968).
- <sup>53</sup>D. Beysens and G. Zalczer, *Phys. Rev. A* **15**, 765 (1977); **18**, 2280 (1978).
- <sup>54</sup>I. Lagues, thesis, University of Paris VI, 1971 (unpublished).
- <sup>55</sup>M. Tournarie, *J. Phys. (Paris)* **30**, 47 (1969).
- <sup>56</sup>H. Klein and D. Woermann, *Ber. Bunsenges. Phys. Chem.* **79**, 1180 (1975).
- <sup>57</sup>I. R. Krichevskii, N. E. Khazanova, and L. R. Lipshitz, *Zh. Fiz. Khim.* **29**, 547 (1955).
- <sup>58</sup>Cited in *Landolt-Börnstein, Eigenschaften der materie in ihren aggregatzuständen -8-Teil-Optische Konstanten* (Springer, Berlin, 1962).
- <sup>59</sup>C. C. Lai and S. H. Chen, *Phys. Lett.* **41A**, 259 (1972).
- <sup>60</sup>The analysis of data from B. Chu's experiments gives the same result (G. Zalczer, private communication, 1980).
- <sup>61</sup>J. Timmermanns, in *Physico Chemical Constants of Lin Solutions Organic Compounds* (Elsevier, Amsterdam, 1965).
- <sup>62</sup>D. B. Myers, R. A. Smith, J. Katz, and R. L. Scott, *J. Phys. Chem.* **70**, 3341 (1970).
- <sup>63</sup>D. Beysens and R. Tufeu, *Rev. Phys. Appl.* **14**, 907 (1979).
- <sup>64</sup>J. H. Hildebrand, B. J. Alder, J. W. Beams, and H. M. Dixon, *J. Phys. Chem.* **58**, 577 (1954).
- <sup>65</sup>H. Klein and D. Woerman, *J. Chem. Phys.* **62**, 2913 (1975).
- <sup>66</sup>G. Morriison and C. M. Knobler, *J. Chem. Phys.* **65**, 5507 (1976).
- <sup>67</sup>S. C. Green and R. Hocken, *J. Chem. Phys.* **63**, 5067 (1975).
- <sup>68</sup>F. Kohler and O. K. Rice, *J. Chem. Phys.* **26**, 1614 (1951).
- <sup>69</sup>D. Atack and O. K. Rice, *Discuss. Faraday Soc.* **15**, 210 (1953).
- <sup>70</sup>A. M. Wims, D. Mc. Intyre, and F. Hynne, *J. Chem. Phys.* **50**, 616 (1969).
- <sup>71</sup>H. B. Tarko and M. E. Fisher, *Phys. Rev. B* **5**, 2668 (1972).
- <sup>72</sup>H. B. Tarko and M. E. Fisher, *Phys. Rev. B* **11**, 1217 (1975).